Yuselis Castaño Guerrero

Lic. Biochemistry

Report of professional activity

Dissertação para obtenção do Grau de Mestre em Bioquímica

FACULDADE DE CIÊNCIAS E TECNOLOGIA
UNIVERSIDADE NOVA DE LISBOA

november 2018

LOMBADA

Report of professional activity
Yuselis Guerrero

2018

Yuselis Castaño Guerrero

Lic. Biochemistry

Report of professional activity

Dissertação para obtenção do Grau de Mestre em Bioquímica

FACULDADE DE CIÊNCIAS E TECNOLOGIA
UNIVERSIDADE NOVA DE LISBOA

november 2018

Copyright

Title: Report of professional activity.

Eu, Yuselis Castaño Guerrero concedo à Faculdade de Ciências e Tecnología e à Universidade Nova de Lisboa, nos terrnos dos regulamentos aplicãveis, 0 direito de divulgar e distribuir copias da dissertaçao.

"A Faculdade de Ciências e Tecnología e a Universidade Nova de Lisboa tém 0 direito, perpétuo e sem limites geográficos, de arquivar e publicar esta dissertação através de exemplares impressos reproduzidos em papel ou de forma digital, ou por qualquer outro meio conhecido ou que venha a ser inventado, e de a divulgar atraves de repositôrios científicos e de admitir a sua côpia e distnibuiçao com objectivos educacionais ou de investigacao, não comerciais, desde que seja dado crédito ao autor e editor'.

Acknowledgements

This professional report involved many people that I would like to thank. First and foremost I would like to thank my actual supervisor Prof. Maria Goreti Ferreira Sales for giving me a chance of being part of Biomark and the opportunity of present this report.

I am grateful as well to Rocio García Miniet, for encouraging me to continue in the research and giving the first oppotunity as research, and well to Maria Elena González Fraguela. I would also thank to Dra. María de los Àngeles Ribas Antúnez for being a great supervisor at my first job. I would also thank to Gerardo González Aguilar for giving me the first opportunity to work in Portugal.

Thank you Robert, Camila, Carolina, Carlos, Daysi, and Carlos Àndres for making my life beautiful and supporting me during all these years.

Abstract

"Biochemistry has become the foundation for understanding all biological processes. It has provided explanations for the causes of many diseases in humans, animals and plants".

Science can improve people's life. It can potentially extend our lives beyond our imagination, and also make our journey more pleasant. In particular life's sciences are in the core of the previous statement. Life's sciences have experienced a huge development in recent years, and it is believed that its impact in society it would be similar in size to that of the physics revolution of the last century, which have lead to some to suggest that this is the "century of biology". This report approach all my professional career from my third year of degree in Biochemistry 2007 to the present research in 2018.

Resumo

"A bioquímica tornou-se a base para a compreensão de todos os processos biológicos. Ele forneceu explicações para as causas de muitas doenças em humanos, animais e plantas".

A ciência pode melhorar a vida das pessoas. Pode potencialmente estender nossas vidas além da nossa imaginação e também tornar nossa jornada mais agradável. Em particular, as ciências da vida estão no centro da declaração anterior. As ciências da vida experimentaram um enorme desenvolvimento nos últimos anos, e acredita-se que seu impacto na sociedade seria similar em tamanho ao da revolução física do século passado, o que levou alguns a sugerir que este é o século. da biologia ". Este relatório aborda toda a minha trajetória profissional desde o terceiro ano de graduação em Bioquímica 2007 até a presente investigação em 2018.

Contents

List of Figures

List of Tables

1 Abbreviations

- POCCA: permanent occlusion of commun carotid arteries.
- SOD: superóxide dismutase.
- CAT: catalase.
- GFAP: glial fibrillary acidic protein.
- MWM: Morris water maze.
- ROS: reactive oxygen species.
- NoV: norovirus.
- RoV: rotavirus.
- AGE: acute gastroenteritis.
- DOXO: doxorubicin.
- BrC: breast cancer.
- Apo: apoferritin.
- ELISA: Enzyme-Linked Immunosorbent Assay.
- HIV: human immunodeficiency virus.
- MIP: molecular imprinted polymer.

2 Introduction

Biochemistry, the "chemistry of life", is synonymous of two older terms: physiological chemistry and biological chemistry. Biochemistry surge as scientific discipline around the early 19th century. Carl Neuberg, an early pioneer, was the fist to propose the term "biochemistry" in 1903.

According to Biochemical Society, "Biochemistry explores the chemical processes within and related to living organisms. The Chemistry of Life concentrates on handling what happens at a molecular level that, what's happening inside the living cells and organelles, studying components like proteins, enzymes, lipids, carbohydrates, DNA and RNA" [1]. Biochemistry describes, in molecular terms, all chemical processes in the living organisms. Biochemistry contains itself a very broad range of scientific disciplines, including molecular biology, genetics, physiology, microbiology-virology, forensics, animal and plant sciences and medicine [2]. Although its ultimate concern is with the wonder of life itself, some of the most exciting questions emerged in the Biochemistry has developed greatly medicine and biology [3].

I'm Biochemistry graduated from the Biology faculty of the University of Havana, Cuba. I started my degree in 2005. My career consist, of five years of academic formation culminating with a thesis. During the first three years I had the opportunity to learn about mathematics, physics, chemistry, biology and all related with biochemistry. At this time I was gaining an interest for molecular biology. During my bachelor thesis, I had the opportunity to work from the molecular level up to the organism level. More specifically, I worked rat models of cerebral hypoperfusion at International Center for Neurological Restoration, Havana, Cuba. This work finished with a publication [4], presented in chapter 3, and it was a big motivation for me as young research.

My contribution in this work was the surgical procedure for implement

permanent occlusion model in rats. I was responsible for characterizing both molecular and behavioral animal models, to test the lesion and control rats group in the behavioral trial Morris water maze (MWM), and make dissections of brain areas for molecular assays. I was responsible too for the oxidative tests, catalase (CAT) and superoxide dismutase (SOD), in this work. This publication was a part of my thesis degree my responsibility, write a big part.

After finishing my undergrad studies, I had the opportunity to work in the Diagnostic Lab of the Institute of Tropical Medicine "Pedro Kourí" in La Habana, Cuba. It is a reference national laboratory in Cuba for confirmation a positive results for dengue, rabies, rubella, measles, mumps, rotavirus (RoV), norovirus (NoV) and human immunodeficiency virus (HIV). In this period I gain knowledge, about viruses and detection methods, including Ultramicro ELISA assay and molecular techniques as RT-PCR and SDS-PAGE. At this time, my main responsibility as young research, was molecular standardization method (RT-PCR) for NoV and RoV detection. I learned how important, is to quickly identify NoV and RoV diseases in children. At this time, we made a study about infection in children caused by NoV and RoV in a cuban hospital, which ended in a published article [5], presented in chapter 4.

Later in 2012, I was accepted in the "Carrera de Especialización en Aplicaciones Tecnológicas de la Energía Nuclear" (CEATEN) course at Atomic Center of Bariloche, Argentina, which aims to bring together multidisciplinary professionals into a single place specializing them in nuclear technologies. Here I learned how nuclear technology is used nowadays in medicine production and therapy of cancer cells.

In 2014, I started to work at INESC-TEC Porto. The first work in this project was a review about Shiga toxin. This toxin create, outbreak, with serious public health, so developing a sensor that could detect it in real time could have a large impact in the outbreak control. This review is presented in appendix A. The goal of this work, to know the state of the art in methods for bacterial detection using biosensors. With this review, we understood that biosensors promise to be rapid, reliable and sensitive detection platforms for bacterial detection. More specifically, during this time, I was involved in the development of a biosensor with the aim to detect bacteria in meals through the detection of *bacillus thuringiensis* and *bacillus cereus*. At this time I learned about the R programming language, through which the results were processed. I also had the opportunity to participate in two international events with a poster presentation. First, at the *"21 Chemistry Conference"* with a poster: *Bacterial threat remote detection using electronic tongues: modeling using Bacillus thuringiensis* in Santiago de Cuba, Cuba. Second,

was the *third SIPS Training School* and *"Third European conference on smart inorganic polymers"* events hold in Porto, Portugal with a poster *Using dye-doped polymer arrays for food contaminant detection.*

More recently in January 2018, I started to work at BioMark, Sensor Research, ISEP, Porto, a project supported by the grant, BIL/IBEROS-BioMark/03. The goal of the job the development of nanomaterials for carrying an antitumor agent, targeting breast cancer. It couldn't be more exciting to work in such cutting-edge research. Up to the current year, we have obtained a very promising preliminary results which points us the next immediate steps to do and also suggest more ambitious goals which we pretend to develop in future project. My role in this research is to develop a nanomaterial carrying on its surface the Trastuzumab and in its interior an antitumor agent (doxorubicin). I was responsible for prepare vehicle which support the drug and encapsulate the DOXO inside of apoferritin. Optimization assays for testing the Dose/response of doxorubicin/vehicle.

This work is organized as follows.

First chapter contains my work in the ischemia model in rats to evaluate the molecular mechanisms that conduce to behavioral disorders, developed from June 2007 until April 2010.

Second chapter is devoted to my work viruses detection, specifically Noroviruses and Rotaviruses, developed from September 2010 until April 2012.

The third chapter contains the progress we made in the project about, development of an electronic tongue for bacterial detection, developed from February 2014 until November 2016.

Fourth chapter describe my recent research about smart drugs delivery, developed from January 2018 until now.

3

Metabolism disorders in a rats model

This chapter is based on [4].

Chronic hypoperfusion in rats produces memory and learning impairments due to permanent occlusion of commun carotid arteries (POCCA). Molecular mechanisms leading to behavioural disorders have been poorly studied. For this reason, the aim of the present study was to characterise oxidative metabolism disorders and their implications in memory and learning impairments. Superoxide dismutase (SOD) and catalase (CAT) activities were determined in cortex, hippocampus and striatum homogenates at 24 hours and at 22 days after the lesion. Haematoxylin-eosin staining and glial fibrillary acidic protein (GFAP) immunoreactivity were performed on coronal sections. Behavioural impairments were explored using the Morris water maze (MWM). Escape latencies were determined in all behavioural studies. The lesion induced a significant increase ($P < 0.01$) in CAT activity in the cortex at 24 hours, while SOD activity was significantly higher ($P < 0.01$) in the cortex and hippocampus at 22 days. An intense vacuolization was observed in the cortex and striatum as a result of the lesion. A neuronal loss in the striatum and hippocampus was observed. The glial reaction increased in the cortex and striatum. Visual alterations were observed in the lesion group with the lowest evolution time ($P < 0.001$). Escape latencies, corresponding to MWM schemes for long-term and short-term memory evaluation increased significantly ($P < 0.05$) in both groups of lesioned animals. It was concluded that changes in SOD and CAT activities indicate, a possible implication of oxidative imbalance in the pathology associated with chronic cerebral hypoperfusion. In addition, the POCCA model in rats is useful for understanding mechanisms by which cerebral hypoperfusion produces memory and learning impairments.

3.1 Introduction

It is a well-known fact that while stroke incidence increases with age, strokes are not necessarily fatal [6]. Ischaemic events occur due to occlusion of a major artery that causes a decrease in blood flow [7] The brain possesses specific traits which make its tissue highly vulnerable to the effects of oxidative stress [8, 9]. An ischaemic event will result in a marked increase in reactive oxygen species (ROS). However, enzymatic antioxidant defence systems found in the brain neutralise such highly reactive species. This defence system relies on cooperative action between intracellular enzymes, which include superoxide dismutase (SOD) and catalase (CAT) [10]. Ischaemia has historically been considered untreatable, and there are no effective treatment options even today [11]. One facet of the search for new treatment therapies focusing on neuroprotection or neurorestoration of the damaged tissue is the development of experimental animal models [12]. The model for permanent occlusion of the common carotid arteries (POCCA) in rats reproduces both the ischaemic event in its early stages and the subsequent oligaemia once cerebral hypoperfusion has become chronic [13]. The hippocampus is part of the brain that has received the most attention from studies on POCCA-induced neuropathological alterations. Cerebral hypoperfusion has been associated with impaired memory and learning; both of these processes involve the hippocampus [12, 13]. It has been suggested that, in addition to the hippocampus, the striatum and the cortex are also highly susceptible to ischaemic events [10]. The purpose of this study is to describe alterations in oxidative metabolism in the cortex, striatum, and hippocampus, and the effect of these changes on memory and learning disorders in a rat model of cerebral hypoperfusion.

3.2 Materials and methods

3.2.1 Experimental subjects

Subjects were male Sprague-Dawley rats from the National Center for the Production of Laboratory Animals (Havana, Cuba). Rats were kept in standard laboratory conditions at a mean temperature of 22°C ± 2°C with a 12/12 hour light-dark cycle and free access to food and water. The established ethical principles for animal research were followed throughout all experiments [14]. Rats had a mean weight of 311g ± 4.37 g at the time the lesion was induced.

3.2.2 Surgical procedure

The 42 rats in the model group were anaesthetised with an intraperitoneal injection of 350 mg chloral hydrate per kilogram body weight. The rats' necks were incised and common carotid arteries were permanently ligated using suture silk 3-0. Rats in the control group (n = 30) were subjected to the same surgical procedure but did not undergo POCCA.

3.2.3 Study of oxidative metabolism

Obtaining biological samples

Following the surgical procedure, at 24 hours (10 experimental, 9 control) and at 22 days (10 experimental, 5 control), the animals were deeply sedated with an intraperitoneal injection of chloral hydrate (700 mg/kg of body weight) and decapitated. Brains were removed so as to dissect areas of the brain (cortex, hippocampus, and striatum) from both hemispheres. Tissues were preserved at -70°C until they were used.

Tissue homogenisation

Areas of the brain were homogenised using a solution of Tris 1 mol/L sucrose 0.25 mol/L with a pH of 7.4 in a homogeniser at 1000 rpm in an ice bath. The product was placed in the centrifuge during 15 minutes at 4°C and 14 000 rpm; the supernatant was preserved frozen at -70°C until it was processed.

Determining superoxide dismutase activity

We used the Marklund method [15] based on the ability of SOD to inhibit the pyrogallol reaction. Delipidation of the samples was performed using an aliquot of 100 μ L of homogenate and adding 30 μ L chloroform and 50 μ L methanol. The mixture was shaken for 1 minute in a laboratory shaker and centrifuged at 4 °C and 3000 rpm for 20 minutes, after which the supernatant was collected. The buffer was Tris 50 mmol/L-HCl 20 mmol/L-EDTA 10 mmol/L with a pH of 8.2. We added 540 μL of the buffer, 30 μL of the sample, and 30 μL of pyrogallol. The mixture was shaken and the optical density (OD) value was obtained from duplicate measurements and recorded as 420 nm at 70 seconds. One unit of enzyme activity was defined as the amount of enzyme necessary to achieve 50 % inhibition of pyrogallol auto-oxidation.

Determining the enzymatic activity of catalase

CAT activity was determined by using Aebi's spectrophotometric method [16] to observe the decomposition of H_2O_2. Our trial used a phosphate buffer (KH_2PO_4 0.12 mol/L-K_2HPO_4 0.12 mol/L) with a pH of 7.4 and a 13 mmol/L H_2O_2 substrate solution in a phosphate buffer. During the trial, 375 μL of phosphate buffer, 204 μL of substrate solution, and 21 μL of homogenate were mixed and shaken. OD values at 240 nm were measured every 2 seconds during 1 minute in a variable temperature cell set to 37°C. OD values were obtained from duplicate measurements. One unit of enzyme activity was defined as the amount of enzyme necessary in order to transform 1 μmol of H_2O_2 in 1 minute at 37°C.

Measuring total proteins

One hundred microlitres each of water (blank sample), a reference sample, and our sample were then mixed with 2.0 mL Bradford reagent (0.1 mg/mL Coomassie blue in 8.5% H_3PO_4 and 4.75% ethanol). OD was measured at 595 nm. Calibration was performed using bovine serum albumin at its extinction coefficient of 280 nm ($k = 0.68mL/mg$).

3.2.4 Evaluation of cell damage

For purposes of the histological study, animals with POCCA (n = 3) and controls with mock lesions (n = 3) were anaesthetised with chloral hydrate 7 days after cerebral hypoperfusion surgery. They received a perfusion of 250 mL 0.9% sodium chloride solution and 250 mL of a 10% formalin flush. Rat brains were placed in an automatic tissue processor (Histokinette). Brains were dehydrated in a series of graded alcohol baths, the alcohol was removed with xylene, and the tissue was subjected to paraffin infiltration. Coronal slices 6 μm thick were stained with haematoxylin and eosin stain and alternately subjected to the procedure for immunohistochemical detection of glial fibrillary acidic protein (GFAP). Slices were treated with 20% fetal bovine serum/Triton X-100 0.25% in a saline phosphate buffer during 30 minutes and incubated overnight at 4°C with polyclonal anti-GFAP antiserum (1 : 500), followed by incubation with biotin anti-mouse IgG1 antibody (1 : 500) for 1 hour at room temperature. Slices were submerged in a streptavidin-biotin-peroxidase conjugate (1 : 100) for 1 hour and the reaction was observed with 0.02% H_2O_2 and 0.05% diaminobenzidine as a chromogen. The reaction was terminated by adding regular water. Slices were dehydrated with a series of graded alcohol baths, rinsed in xylene, and observed under an optical

microscope.

3.2.5 Evaluation of behaviour disorders

The Morris water maze (MWM) is a procedure in which researchers measure the time it takes animals to locate a platform measuring 11 cm in diameter, whether it is visible or hidden, in order to escape from a pool of water (escape latency). Each rat was given a maximum of 60 seconds to search for a way out of a circular tank 1.5 m in diameter and filled with water to a depth of 40 cm. A camera trained over the centre of the water tank enabled data acquisition, and data were processed using SMART software version 2.0, copyright Panlab, 2001.

Behavioural tests were conducted in 2 different phases: in 1 group of animals at 18 days post-lesion (model group n = 9, mock lesion group n = 8) and in the other group at 33 days post-lesion (model group n = 10, mock lesion group n = 5).

Evaluating sensorimotor and motivational deficits

The platform was placed so that it was visible, and each rat completed 8 trials at 22 and 37 days post-lesion. Each trial began by placing the rat at a randomly selected position along the perimeter of the tank.

Evaluating long-term or spatial reference memory

In this test, which was conducted between days 18-21 and days 33-36 post-lesion, the rats had to find the platform, now concealed, at its previous location. Each rat had 29 trials (8 trials in the first 3 days and 5 trials on the last day).

Evaluating short-term or working memory

Spatial reference memory was tested at 33-35 and at 48-50 days after injury. Animals were tested during 3 days, and the position of the hidden platform was changed every day. The 4 trials were conducted in 3 days; the time elapsed between a trial and the following one was 20 seconds at first, followed by 20 minutes, and finally followed by 2 hours.

3.2.6 Statistical method

The recorded data were processed using professional software: Statistica for Windows, version 6.0, Copyright Statsoft Inc., 1996. Values were shown as

the mean ± standard error of the mean. We determined whether or not the data were normally distributed using the Kolmogorov-Smirnov test. Since the Levene test did not reveal homogeneity of variance, we performed a non-parametric data analysis.

Comparisons of antioxidant enzymes between animals in the mock lesion group and those in the model group were performed using the Mann-Whitney U-test. The same test was used to compare results from behavioural tests in the control group and in the mock lesion group, and between animals in the experimental group at different points in time. The Wilcoxon rank-sum test was used to compare behavioural task performance by the same group of animals at different times.

3.3 Results

3.3.1 Oxidative metabolism

There were no significant differences in antioxidant enzyme activity between animals in different control groups, so all control groups were considered to be the same.

At 24 hours after occlusion, there were no variations in SOD activity in any of the brain areas that were studied (Fig. 3.1). There was a significant increase in SOD activity in the cortex and hippocampus at 22 days post-lesion ($P < 0.001$). On the other hand, animals with cerebral hypoperfusion at 22 days post-lesion also showed a significant increase in enzymatic activity in the 3 areas of the brain that were studied ($P < 0.05$) compared to animals that were euthanised at 24 hours post-lesion.

The POCCA procedure led to increased CAT activity at 24 hours, but this increase was only significant in the cor- tex ($P < 0.01$) (Fig. 3.2). At 22 days after carotid occlusion, this increase was no longer statistically significant.

3.3.2 Evaluation of cell damage

We observed pronounced vacuolisation in the cortex and striatum. However, decreases in neuronal density were only recorded in the striatum and in the CA1 and CA3 populations of the hippocampus (Fig. 3.3).

Animals with cerebral hypoperfusion displayed an increase in glial markers in the cortex and the striatum,with decreased glial response in CA1 and CA3 cells compared to control animals (Fig. 3.4).

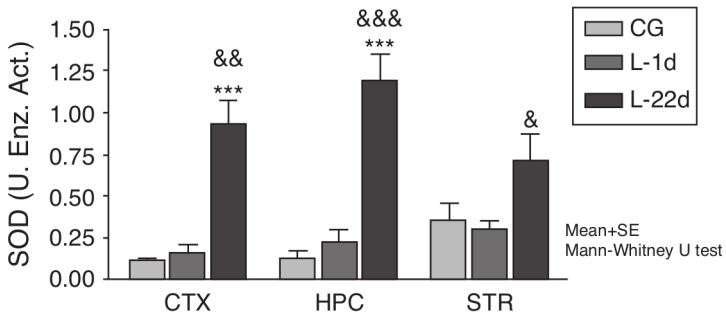

Figure 3.1: Activity of superoxide dismutase in the cortex, hippocampus, and striatum of rats subjected to permanent occlusion of common carotid arteries. The graph shows enzyme activity among model group animals at 22 days post-lesion compared to the control group ($***P < 0.001$) and the model group at 24 hours post-lesion ($\&P < 0.05; \&\&P < 0.01; \&\&\&P < 0.001$). Bars represent mean values ± standard error of the mean. CTX: cortex; STR: striatum; CG: control group; HPC: hippocampus; L-1d: group at 24 hours post-lesion; L-22d: group at 22 days post-lesion; SOD: superoxide dismutase.

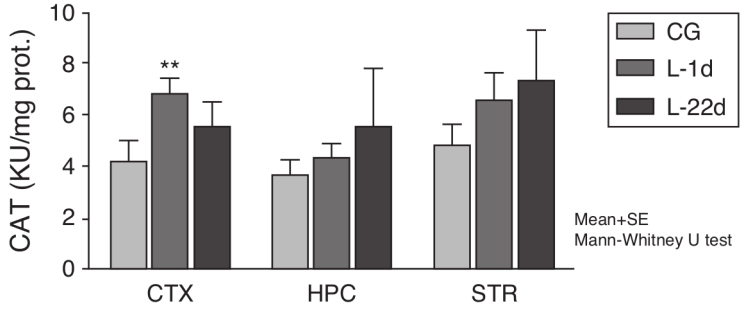

Figure 3.2: Activity of catalase in the cortex, hippocampus, and striatum of rats subjected to permanent occlusion of common arotid arteries. The graph shows enzymatic activity in model group animals compared to control group animals ($** P < 0.01$). Bars represent mean values ± standard error of the mean. CAT: catalase; CTX: cortex; STR: striatum; CG: control group; HPC: hippocampus; L-1d: group at 24 hours post-lesion; L-22d: group at 22 days post-lesion.

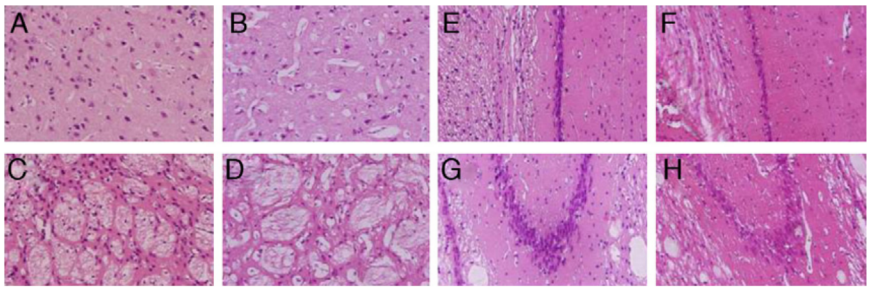

Figure 3.3: *H&E* stains of coronal slices of the cortex (A and B), the striatum (C and D), CA1 (E and F), and CA3 (G and H) at 40X magnification. Columns on the left show slices taken from control-group animals; columns on the right show sections from animals with cerebral hypoperfusion at 7 days post-lesion.

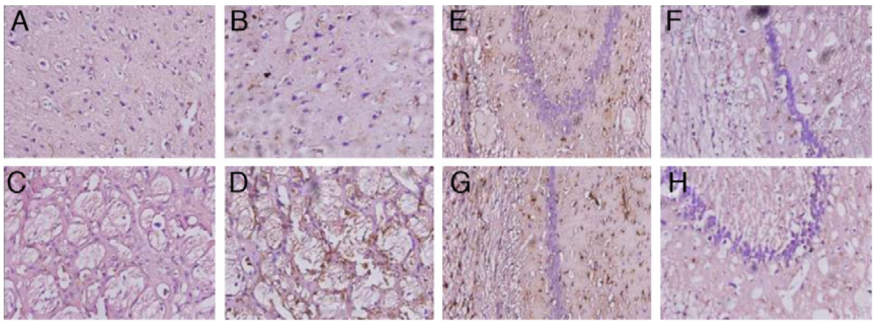

Figure 3.4: Microphotographs showing coronal slices from rat brains with glial fibrillary acid protein immunostaining in the cortex (A and B) the striatum (C and D), CA1 (E and F), and CA3 (G and H) at 40X magnification. Columns on the left show slices taken from control-group animals; columns on the right show sections from animals with cerebral hypoperfusion at 7 days post-lesion.

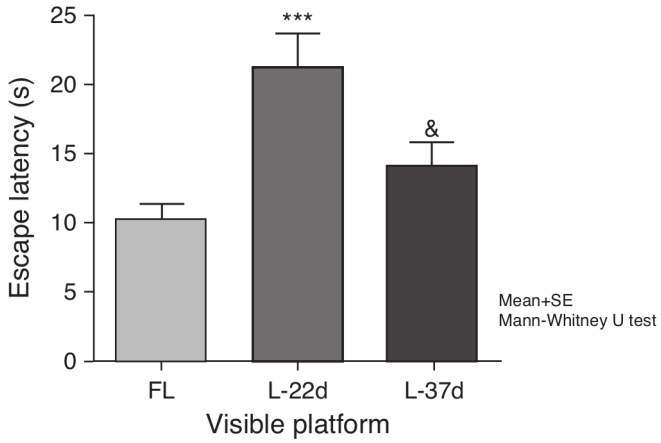

Figure 3.5: Influence of chronic cerebral hypoperfusion on sensorimotor and motivational deficits. For this task, the escape platform was visible. $***P < 0.001$: escape latency in the model group at 22 days post-lesion was longer than in the control group. $\&P < 0.05$: escape latency in the model group at 37 days post-lesion was shorter than in the model group at 22 days post-lesion. Bars represent mean values ± standard error of the mean. CG: control group; L-22d: group at 22 days post-lesion; L-37d: group at 37 days post-lesion.

3.3.3 Behavioural trials

Control groups matched to model groups for different times post-lesion displayed no significant differences on any of the behavioural tests. All of these control groups were therefore considered to be a single control group.

Sensorimotor and motivational deficits

Animals with cerebral hypoperfusion assessed at 22 days post-lesion required a significantly longer time to find the escape platform than control animals did ($P < 0.001$). At 37 days after carotid occlusion, these differences were no longer statistically significant. The animals at more advanced post-lesion stages required significantly less time to find the platform than animals which had been experiencing cerebral hypoperfusion during a shorter time period ($P < 0.05$) (Fig. 3.5).

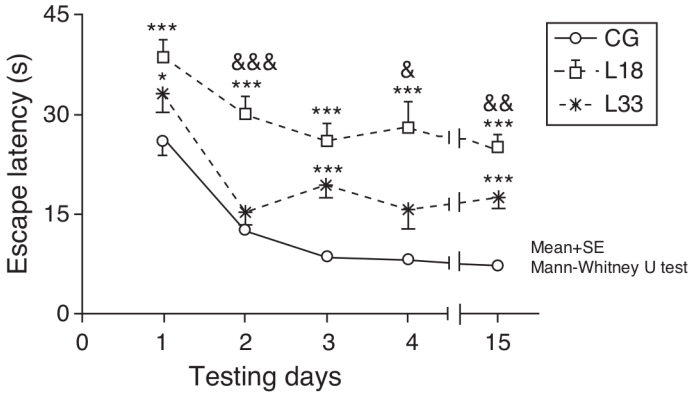

Figure 3.6: Evaluating long-term or spatial reference memory. In this trial, the platform remained at the same location, but was hidden. Values show mean escape latencies ± standard error of the mean. $*P < 0.05 : ***P < 0.001$: escape latencies from both model groups compared to control group. $\&P < .05; \&\&P < .01; \&\&\&P < .001$; differences between escape latencies in both model groups. CG: control group; L18 and L33: animals that began testing at 18 days and 33 days post-lesion.

Long-term or spatial reference memory

A long-term memory assessment revealed that animals in the study decreased their escape latency period as the days passed ($P < 0.05$). Performance by rats with cerebral hypoperfusion at 18 days post-lesion differed significantly from that of control-group animals ($P < 0.001$). Escape latency in animals at 33 days post-lesion was longer than in control-group animals and the differences were statistically significant for the first, third, and last testing days ($P < 0.05$). Therefore, animals with cerebral hypoperfusion in earlier post-lesion stages showed escape latencies that were significantly longer than animals at 33 days post-lesion on the second, fourth, and last testing days ($P < 0.05$) (Fig. 3.6).

Short-term or working memory

Escape latencies in rats at 33 days post-lesion was significantly longer than latencies in the mock-lesion group for all 3 testing days (Fig. 3.7) ($P < 0.05$). Animals evaluated at 47 days post-lesion showed significant differences in the final 2 testing days ($P < 0.05$). Comparison of escape latencies among the model groups revealed that latencies were shorter in the group at the most advanced post-lesion stage. However, this difference was only statistically

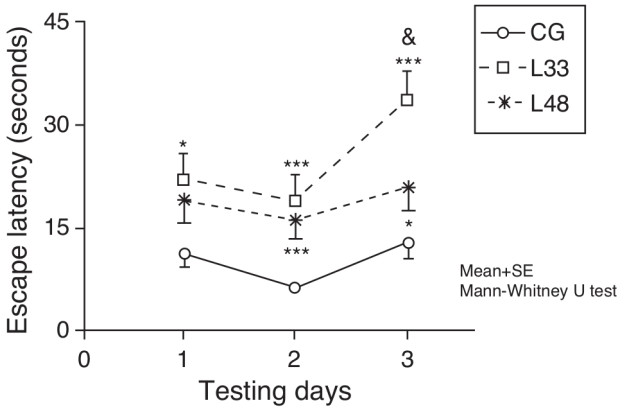

Figure 3.7: Short-term memory impairments as a result of chronic cerebral hypoperfusion. Points along the curve correspond to mean values ± standard error of the mean. $*P < .05; ***P < .001$: indicates that escape latencies in the model group were longer than in the control group. $\&P < .05$: shows differ- ences between different model groups. CG: control group; L33 and L48: animals that began testing at 33 days and 48 days post-lesion.

significant for testing day 3 ($P < 0.05$).

3.4 Discussion

In ischaemic and oligaemic processes, the generation of reactive oxygen species takes place as a result of decreased blood flow to the brain [17,18]. Our studies show that SOD activity did not change in response to acute cerebral hypoperfusion; however, the enzyme was extremely sensitive to chronic cerebral hypoperfusion at 22 days post-lesion. At 24 hours post-lesion, the 3 areas of the brain studied here experienced a marked decrease in blood flow, [19] which was accompanied by an abrupt decrease in oxygen supply. This fact, added to reperfusion in this model being gradual and very slow, results in the production of only small amounts of superoxide radicals. It is therefore likely that xisting SOD is sufficient to eliminate those superoxide radicals. However, at 22 days after POCCA was induced, most of the cerebral blood flow had been restored. As a result, the brain had a better oxygen supply and increased formation of superoxide radicals, which was sufficient to induce SOD activity.

The protective effect of SOD can only be achieved with the consecutive participation of another 2 enzymes that degrade H_2O_2 : CAT and GPX [20]. In our study, the increase in CAT activity was only significant in the cortex

24 hours after the lesion. This increase in CAT activity took place despite the lack of a parallel increase in SOD activity, which would normally occur with reperfusion [10]. This behaviour can be explained if we consider the possible presence of an accumulation of H_2O_2 which would be accompanied by an increase in CAT activity. If H_2O_2 is able to accumulate, it may demonstrate that this molecule is stable and able to cross membranes. Furthermore, since reperfusion does not take place suddenly, circulating H_2O_2 is not eliminated and continues accumulating.

Despite the marked increase in SOD activity in the 3 areas of the brain we studied, we did not identify any significant increases in CAT activity at 22 days post-lesion. Although some in vitro studies show that CAT is essential for intraneuronal H_2O_2 detoxification, the activity of this enzyme in the nervous system has been proven to be very low [21, 22]. It is therefore likely that GPX metabolises most of the H_2O_2 that forms as a product of SOD activity.

The haematoxylin and eosin stain is the most commonly used staining method in histology. The extensive vacuolisation observed in the cortical tissue and striatum of animals that were euthanised 1 week after POCCA resembles that described in other studies published in the scientific literature [23, 24]. Furthermore, we observed a decrease in neuronal density in the striatum. Neuronal loss in the CA1 and CA3 cell populations of the hippocampus in our study, induced by cerebral hypoperfusion, is coherent with results from other studies [25–27].

The reactive astroglioisis found in the cortex of rats with cerebral hypoperfusion supports findings from the study by Schmidt-Kastner et al. [28]. These authors believe that reduced blood flow in the cortex results in a deficient supply of substrates to the neurons, and that neurons may then induce an astrocyte response. On the other hand, reactive gliosis may occur in answer to a neuronal loss that favours the stimulation of restorative processes in brain tissue, such as the synthesis and release of neurotrophic factors [29]. In keeping with this line of reasoning, we discovered a considerable increase in both the size and the number of glial cells in the striatum of the injured rats.

The decrease in GFAP expression associated with the CA1 and CA3 cell populations in the hippocampus corresponds to findings published previously in the literature [30]. Astrocytes present different responses to ischaemic events depending on damage magnitude and duration [31]. Some have theorised that astrocytes proliferate during early stages of ischaemia, but when the period of hypoperfusion is prolonged, they suffer progressive degeneration [32].

The rat model of cerebral hypoperfusion has mainly been associated with

neurodegeneration of the hippocampus. The escape latencies for the lesion group in the trial with the visible platform at 22 days post-lesion suggest an impaired ability to locate visual stimuli. This hypothesis is supported by a number of studies showing that cerebral hypoperfusion results in degeneration of the optic tract, retinopathy, and loss of pupillary reflex [12, 27, 33].

Animals with chronic cerebral hypoperfusion at 37 days post-lesion had no difficulty in locating visual stimuli, as demonstrated by the lack of significant differences between the latency periods of animals in the experimental and control groups. This indicates that visual impairment improves as time elapses following the lesion. This finding may be associated with the activation of adaptive mechanisms that restore blood flow levels. Scientists have demonstrated that cerebral hypoperfusion leads to an increase in diameter in the arteries linked to the circle of Willis, which include the basilar artery, the posterior cerebral artery, and the posterior communicating artery [28, 34].

Analysis of results from the MWM tasks evaluating spa- tial reference memory reveals that animals in both groups were able to learn the location of the platform. This is corroborated by the significant decrease in escape latency over the days during the testing period. Our results indicate that chronic reduction of cerebral blood flow compromises spatial reference memory, as other authors have also concluded [30, 35, 36]. We must not lose sight of the fact that the animals' performance on MWM tasks depends on their being able to locate visual clues outside of the maze itself. This is why the visual system impairment occurring in this model elicits poorer performance of this task. However, in this study we did observe an improvement in spatial reference memory among animals in the model group as post-lesion time elapsed. Improvements were parallel to those observed for the visible platform task. This finding suggests that, in tests performed after a longer period of oligaemia, behavioural results may reflect changes in memory and learning processes.

POCCA also induces changes in short-term (working) memory. Animals tested after a longer period of oligaemia performed better than those tested after a shorter period. We feel that this behaviour is due to results from tests in earlier post-lesion phases being affected by the animals' visual impairment.

In the tests performed by animals that had experienced oligaemia for longer periods, the increases in escape latency were only significant on the second and third testing days. This behaviour is associated with the time elapsed between one trial and the next for each of the testing days. On the first day, the intertrial interval was only 15 seconds, meaning that the animal had less difficulty finding the platform.

3.5 Conclusions

One hypothesis is that the formation of free radicals is a mechanism contributing to neural impairment [37]. Our study demonstrates the existence of an oxidative imbalance in response to chronic cerebral hypoperfusion in the hippocampus, striatum, and cortex. These regions are especially vulnerable to the generation of ROS [38]. This finding suggests that the formation of free radicals may be partially responsible for the ongoing cellular damage which characterises the areas of the brain studied in our experimental model [30].

On the other hand, we also know that cognitive functions are housed in specific neural circuits which in some cases may span wide areas of the brain. A number of cortical zones, together with the amygdala and the striatum, participate in gathering the information. Some of this information is transferred to the hippocampus. The CA1 and CA3 areas participate in creating short-term memories and transfer this information to the neocortex, which stores it for longer time periods [29]. On this basis, we might say that neuropathological changes associated with cerebral hypoperfusion in the POCCA model underlie the deterioration of memory and spatial learning processes.

Animal models for cerebral ischaemia began to be used in the 1970s. The purpose of such models was to enable study of damage caused by cerebral ischaemia under physiologically controlled, repeatable conditions [39].

The pathophysiological processes in cerebral ischaemia result from a series of cellular and molecular phenomena taking place over both the short-term and the long-term. They converge in 2 modalities of cell death: necrosis and apoptosis (programmed cell death). Our understanding of these mechanisms is growing, and this is fundamental to the implementation of neuroprotective strategies in clinical practice. Basic knowledge of the pathophysiology of ischaemia and of microglial and macroglial responses is necessary in order to plan neuroprotective strategies. Such strategies must be designed to prevent both acute cell death and later-onset cell death modalities, and also strengthen surviving tissue. Promising neuroprotective drugs are becoming available, and they are being studied in both experimental animal models and in clinical trials in humans [7].

Different phases have been suggested for neuroprotective strategies, depending on which molecular event is the target of the intervention. Experimental studies enabling molecular characterisation and establishing time windows for such interventions are available and may be consulted for further information. Neuroprotective strategies are based on detailed knowledge of each of these phases, and scientists search for key events that may be tar-

geted by pharmacological or physical interventions aimed at limiting neuronal damage and facilitating recovery [7]. With this in mind, the rat model of induced cerebral hypoperfusion may be useful for evaluating the efficacy of neurorestorative, neuroprotective, and antioxidant therapeutic strategies that promote recovery of cognitive functions.

The main purpose of studies carried out using experimental models of cerebral ischaemia must be to compile basic knowledge about pathobiological processes underlying ischaemic injury. These studies should not be used merely to demonstrate treatment benefits as a preliminary step in the design of clinical trials [39].

4 Norovirus and Rotavirus detection

This chapter is based on [5].

4.1 Introduction

Norovirus (NoV) and Rotavirus (RoV) are the major cause of outbreaks and sporadic gastroenteritis worldwide. NoV has become the leading cause of acute gastroenteritis (AGE) in all age groups [40]. The aim of the study was to identify NoV infection, to know the clinical characteristics and its association with RoV infection in children aged less than five years hospitalized at the Havana Centre Paediatric Hospital, Havana, Cuba, due to AGE, from March 2010 to February 2011.

4.2 Materials and methods

Eighty-eight stool samples collected from children aged less than five years were studied. RoV and NoV antigens were detected by ELISA (IDEIA TM Rotavirus, OXOID Ltd., United Kingdom) and RT-PCR respectively [41]. The SPSS programme (SPSS Inc., Chicago, IL) was used for the statistical analysis.

4.3 Results

Fifty-four samples (61.4%) turned out positive for RoV and 31.8% (28/88) were positive for NoV ($p > 0.05$). Infections of RoV were seen in 51.9% of male children (28/54), whereas NoV infections were observed in 53.6% (15/28) of female patients ($p > 0.05$).

	Rotavirus positive (n = 54) %	Norovirus positive (n = 28) %
Age (months)		
1–6	13 (24)	5 (17.9)
7–12	31 (57.4)	18 (64.3)
13–24	9 (16.7)	4 (14.3)
25–60	1 (1.9)	1 (3.6)
Gender		
Male	28 (51.9)	13 (46.4)
Female	26 (48.1)	15 (53.6)
Fever	41 (75.9)	20 (71.4)
Diarrhoea	53 (98.1)	28 (100)
>3 episodes/24 h	44 (81.5)	22 (78.6)
Vomiting	37 (68.5)	14 (50)
>3 episodes/24 h	26 (48.1)	10 (35.7)
Triad (vomiting, diarrhoea, fever)	34 (62.9)	17 (60.7)

Table 4.1: Clinical characteristics of Norovirus and Rotavirus infection, in children under 5 years old.

Among positive patients, NoV genogroup GII was the most prevalent, detected in 78.6% (22/28). Mixed infections were identified in 20.5% patients (18/88).

The peak incidence of infection (RoV/81.5%; NoV/82.1%) was in children under 12 months. No death was reported.

The clinical features of patients with RoV and NoV infections are displayed in Table: 4.1. RoV positive cases had more episodes of diarrhoea in 24 h (81.5%) than cases of NoV infection (78.6%).

4.4 Discussion

Clinical sings and symptoms were not different between RoV and NoV case-patients. However, fever (41/75.9%) and vomiting (37/68.5%) were more common in RoV compared to NoV infection (fever- 20/71.4%; vomiting-14/50%) ($p > 0.05$). The classic triad of symptoms (diarrhoea, vomiting, and fever) occurred in 62.9% of RoV and 46.4% of NoV infected children.

RoV and NoV were detected year round; however, the infection peaked in the months from December to February: 62.9% (34/54) and 60.7% (17/28)

of RoV and NoV respectively.

In conclusion, it was found that RoV continues to be a common etiological agent of diarrhoea in hospitalized children aged less than five years, as has been reported previously [42, 43]. However, the laboratory limitations to detect sporadic cases of NoV in paediatric hospitals, underestimate diagnosis of this infection.

Of the NoV genogroups, GII was predominant, which was consistent with studies conducted in other settings [44].

A seasonal pattern of RoV and NoV was not noted, because samples were not collected every month. Clear seasonality in RoV infection in the country has not been demonstrated, although a high frequency has been found during winter months [40, 42].

4.5 Conclusions

In the study, RoV and NoV clinical characteristics were mostly indistinguishable, although some authors consider vomiting associated to NoV infection more frequently [40, 44].

Mixed infection among RoV and NoV was observed in children aged less than one year. Different factors can cause infection in these children, as early breastfeed replacement and the hygienic measures taken by adults who work with children [44].

This study confirms the importance of NoV and RoV infection in hospitalized children aged less than five years. Further studies integrating other virus in the diagnosis of AGE need to be undertaken.

5

Bacterial threat remote detection using electronic tongues

Bacteria, viruses and other microorganisms are responsible of many infectious disease which are widely distributed in all world. The incidence of human disease caused by foodborne pathogens increase annually. The traditional methods to bacterial detection are not effective, are laborious, relative time-consuming, expensive equipment and trained personal. Alternatively to conventional platforms for pathogens detection have been recently considered the biosensors, due to high grade of sensitivity and detection specificity, miniaturization and portability to real-time monitoring. Specifically, the concept of electronic tongues is gaining attention through the possibility of, multiples sensors to minimize the errors regarding the use of sensor. The *Bacillus thuringiensis* is an insect pathogen with application in biological control and are not known to cause disease in human. Therefore, has been used as non pathogenic organism in the development of biohazard models. In our work *B. thuringiensis* strains, as model of *B. cereus* to construction of electrodes multiples with similarities among them in chemical composition. The electrodes response detection was with an arduino connected to micro PC (Raspberry Pi), which have a program capable to show the measure from each electrode. The data access is remotely through a normal internet connexion from a control center. Thus, is possible, create an epidemiological monitorization network without the use of periodic sampling at distant sites.

5.1 Introduction

The infections by microorganisms are found widely distributed. Bacteria, viruses and other microorganisms are responsible many infectious disease.

The microbial disease is a major cause of death in many developing countries. The incidence of human disease caused by foodborne pathogens increase annually. The effective detection of bacteria requires methods of analysis where the time and sensitivity is the fundamental limitation for these testing [45].

It is considered that an appropriate response to bacterial outbreaks consist, in its early detection and the use of adequate antibiotics to control them. Typically, the traditional methods involve a series of steps: preenrichment, selective enrichment, biochemical screening and serological confirmation. This process is laborious, relative time-consuming, expensive equipment and highly qualified technical staff are required [46]. Pathogen diagnostics requires of rapid detection, quantification and report of a multitude of different analytes simultaneously. The development of new techniques is important to provide an efficient and quick diagnostics. In this context, biosensors can be particularly useful giving its versatility and it is important to build biosensors capable to obtain multiple and larges amounts of datas and with a low signal-to-noise ratio. Biosensors require traduction elements capable to process multiple analytes separately in fact these biosensors demand sophisticated fabrication technology. Nevertheless, many studies suggest only to detect single compounds [47].

Biosensors have been recently considered as attractive alternative to conventional platforms for pathogens detection because they have superior characteristics. High grade of sensitivity and detection specificity, minimum effort in sample preparation, profitability, miniaturization and portability to real-time monitoring, while reducing the total time requested for detection. Therefore, a great effort has been allocated, the development of rapid biosensors of diverse nature, as they are considered promising devices for pathogenic bacteria detection [46, 48].

Biofabrication technologies for biosensors applications have been advancing and especially involving novel materials or combinations of materials. The advances most applicable to biosensors are print, and deposition technologies. For the building of biosensors of high-throughput, typically is deposited a molecule of interest a strate, and is measured the bind, of another molecule or cell. Three elements biosensors: the biological signal (analyte), the transducer(s), and the detector/readout. First occurs the biological signal, and the engineering parts (transducer and detector) transforms a biological changes in a measured signal for analysis [47].

Specifically, the concept of electronic tongues is gaining attention through the possibility of multiples sensors to minimize the use errors regarding the use of unique sensor. The electronic tongue is a new concept in the world of chemical biosensors. According to Del Valle, 2011 electronic tongues are defined a multisensor system, which consists of a number of low-selective sen-

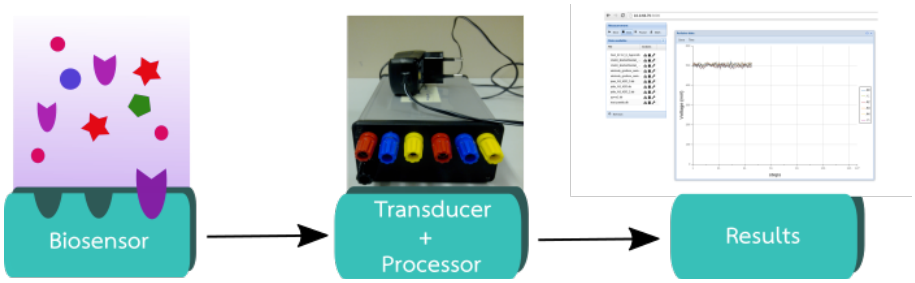

Figure 5.1: Experimental configuration: The electrode recognize the bacillus of the sample. The biosensor signal is detected with an arduino which is connected to Raspberry Pi. The results is shown with a "Data Collector" program.

sors and uses advanced mathematical procedures for signal processing based on Pattern Recognition and/or Multivariate data analysis—Artificial Neural Networks (ANNs), Principal Component Analysis (PCA), and so forth [49].

Bacillus anthracis, Bacillus cereus and *Bacillus thuringiensis* have genomic content in correspondence with a single species but possess diverse virulence properties [50]. The *Bacillus thuringiensis* is an insect pathogen with application in biological control and are not known to cause disease in human. Therefore, has been used as non pathogenic organism in the development of biohazard models, more specifically have been used as an outdoor simulant of anthrax. This is not a novel idea but has been adopted because it facilitate the experimental studies with biohazard organism [51]. We used B. thuringiensis strains as model of B. cereus to construction of electrodes multiples with similarities among them in chemical composition.

The aim of our work is to obtain a preliminary configuration to detect *B. thuringiensis* (fig: 5.1). In our work the electrode signals obtained with an arduino connected to a micro PC, which have a program developed for us to show the measure from each electrode. The Arduino is an open source-low cost electronic platform based on a simple microcontroller board, and a development environment, designed to facilitate the use of electronics in multidisciplinary projects. Arduino can take information from the environment through its analog and digital inputs. The projects made with Arduino can run without connecting to a computer [52]. The micro PC is a Raspberry Pi, which is believed to be an ideal learning tool, that it is cheap to make and easy to replace. A little computer can be used in electronics projects and it is an ideal product to jumpstart computing in the developing world [53].

5.2 Materials and methods

5.2.1 Bacillus Thuringiensis Preparation

Bacillus thuringiensis (Bt): 4 mg of Bt is resuspended in 5 ml of distilled water. Working solution of $0.2mg/ml$ equivalent to $3x10^7 spores/ml$.

For bacteria/spore recognition the imprinted is made at the surface. Briefly, on a acetate dish, of the same diameter of the electrode is poured a drop of gelatin. After gelatin solidification the solution of the target is poured on top of the obtained gelatin structure. The prepared surface is poistioned on a electrode containing the polymeric mixture.

5.2.2 Electrode Preparation

The working electrodes were prepared onto of copper disc of 100 μm thick. The electrodes were fabricated as follows: the activated carbon and superglue were mixed and with this carbon paste was coated the copper disc and was formed the electrode body. The electrode body made with the carbon paste it was left to dry at 50°C in an oven for overnight. Over carbon was deposited a vinyl solution prepared with: 0.15 ml of Vinyl Acetate ($C_4H_6O_2$), 0.15 ml of Ethyl Vinyl Ether (C_4H_8O), 0.4 ml of Styrene (C_8H_8), 0.15 ml of 4-Vinylpyridine (C_7H_7N), and as reactor activator the 1 mg of Benzoyl peroxide ($C_{14}H_{10}O_4$), all the reactive was obtained from Aldrich.

Immediately after to deposited the vinyl solution the *Bacillus thuringiensis* preparation was immobilizated on the electrode surfaces. The electrodes was drying and after was washing with distilled water.

5.2.3 Data Acquisition

Data acquisition was made with an low cost acquisition card Arduino Leonardo (www.arduino.cc). This card was programmed with an sketch with convert it into a serial listener client for a Raspberry Pi (www.raspberrypi.org) small format personal computer. The sketch written fo the Arduino card answer the query sent by the PC, which in this case is just to measure the sensor(s) voltage. The Raspberry runs a server written in node.js wich sends a command to the Arduino card, receiving its data and then the data are saved to a sqlite3 database and at the same time broadcasted through a TCP port to the network.

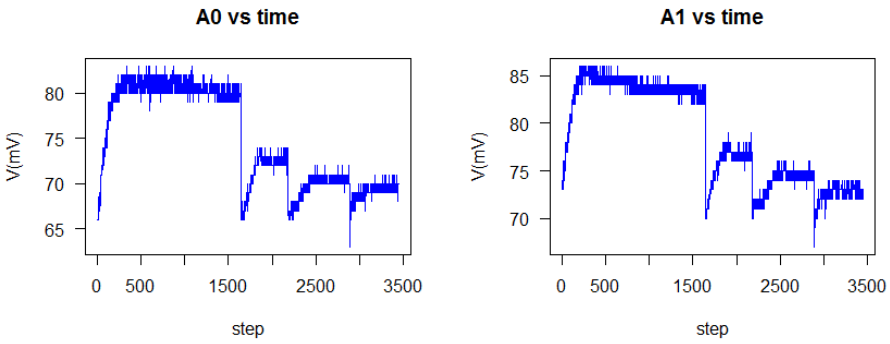

Figure 5.2: Electrodes signal Voltage vs time for B.thuringiensis additions.

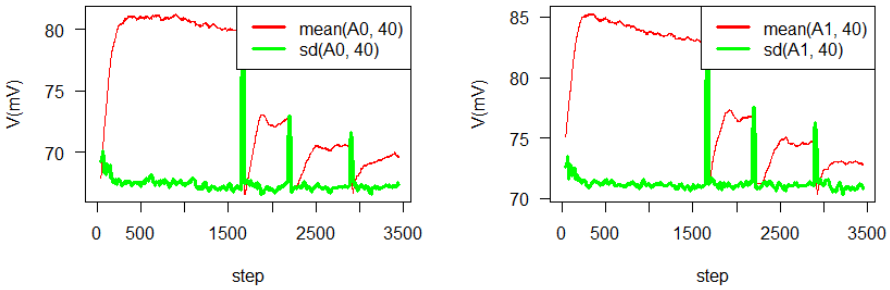

Figure 5.3: Electrodes signal with Kalman filter and the running mean to filter the signal

5.3 Results

The fig. 5.2 shown two electrodes signals (A0 left, A1 right). The graph of voltage of electrodes vs time shows a jump at the addition time.

The arduino board has an unique A/D conversor. For electronical reasons, reading 8 port with only one conversor introduces some noise. To supress that noise, a Kalman filter and the running mean were use to filter (smooth) the signal.

The figure 5.3shows the result of using a Kalman filter above and a running mean down. The figure down also shows the running mean and the peak appear in the spore additions.

5.4 Discussion

We have preliminary results in the electrodes response for *B.thuringiensis* detection. This particular disposal was able to find the spore additions.The staircase graph is the plotting of the concentration against time and shown each jump was the signal was in response of spores additions. The sensor A0 and A1 correlates well each other, allowing to evaluate the reproducibility of the method.

The data was observed remotely, its was able to be observed from several computers at the same time. These results were visualized with an http interface which can be shown through any browser as Mozilla Firefox or Google Chrome in Windows or Linux without problems.

This interface was build using the popular JavaScript library Ext JS and currently allows to see real time graph of voltage of electrodes vs time, and to save, rename and delete the measured data.

This setup offers the possibility to acquire data from several arduino cards at the same time, being able to construct a network of hundred of sensors inexpensively. In fact, some tests were also conducted with an STM32F4 discovery kit, as substitutes of the Arduino card, using the same node.js server obtaining promissing results. The amount of sensors connected simultaneously to the arduino card were from four to six for each experiment.

5.5 Conclusions

These preliminary results, shown that a simple and cheap configuration can be used for the pathogen reproducibility of the electrodes and how a simple processing tool: the running mean, is able to find the spore additions.

The Data Collector program is able to maximize the accesibility of the data through mutiple devices and operative systems, as the client only need a web browser installed to function.

6 Smart nanomaterials for drug-delivery

Breast cancer is leading the statistics of cancer diseases in women. Although chemical treatments are improving within time, their well-known secondary effects sustain the need for (novel) targeted therapies. Cancer cell targeting research is therefore a field under continuous expansion. The targeting element is obviously critical in this context. Humanized monoclonal antibodies primary choice in this context, currently used in clinical context. As proof-of-concept, this approach is applied to track HER2+ breast cancer receptors, employing a carrier of apoferritin (Apo) containing doxorubicin (DOXO).

6.1 Introduction

Breast cancer (BrC) is the most common cancer diagnosed among women [54], being the second cause of death around the world [55]. Despite the existing techniques for its early detection, the global mortality remains high. BrC can be classified by the expression of cell-specific biomarkers into differents groups: estrogen receptor (ER), progesterone receptor (PR) and human epidermal growth factor receptor-2 (HER2) [56]. Although HER2-positive cancer is not the most abundant form of BrC, it is aggressive and fast-growing, requiring quick and effective responses. This form of cancer is characterized by an overexpression of the HER2 receptor [57], which is related to its severity and drug response [58]

BrC therapy relies mostly in chemotherapy and radiotherapy, which may effectively kill tumour cells but also harm normal cells. Targeted cancer therapy emerged to improve this scenario, by using specific nanomaterials in drug delivery targeting [59]. The elements to be targeted are usually cell specific receptors, thereby increasing the affinity of the carrier to the cancer

cell, leaving normal healthy cells unharmed. This approach became more effective and less toxic for cancer patients than conventional therapy [56].

DOXO is a anthracycline antibiotic used frequently alone or with other drugs as treatments in several differents types of cancer, and have showed, be effective [60]. Its usage as conventional medication limited due to the cardiotoxicity adverse effect. A novel idea for decreased DOXO-related toxicity is the use of carrier systems. Thus, development of drug-delivery systems represents a successful strategy to limited the exposure in sites frequently associated with conventional anthracycline toxicity, such as the myocardium [61]. Many authors report, that the determinants in the DOXO cardiomyopathy is the cumulative dose. The use of smaller and divided doses decrease the likelihood of developing heart failure [62].

Many therapeutic solutions have been focused in the development of nanoparticles for drug delivery targeting [59]. As targets for drugs delivery are used cell-specific biomarkers, like monoclonal antibodies, non-antibody proteins and other molecules [56].

The vehicle supporting the drug and the targeting element should offer biodegradable and biocompatible features and undergo a rapid and complete metabolism and elimination after their in vivo activity. The most common drug delivery, are recurrently based on inorganic materials, organic matrices or hybrid (inorganic/organic, core/shell) structures. Alternatively, the protein-cage molecules based on ferritins is emerging as an effective way to carry drugs. Ferritins have exceptional characteristics, namely biodegradability, solubility, functionalization versatility, and remarkable capacity to bind different types of drugs [63, 64].

Apoferritin (Apo) has the ability to self-assemble: disassembles into subunits at pH < 3.0 and reassembles as an intact sphere at pH > 5 [63]. Thus, using the iron empty cavities of Apo nanocage [65], DOXO can be loaded inside the nanocarriers by a reassemble route involving pH variations [63].

In the present work we intend to develop a nanomaterial carrying in its interior DOXO as model antitumor agent. This is herein tested in HER2+ breast cancer (fig. 6.1).

6.2 Materials and methods

6.2.1 Materials and instruments

The biological material used was MCF7 cell line from human breast (adenocarcinoma). The chemical, used were ferritin equine spleen Type I (Sigma Aldrich), Sodium acetate (Riedel-de-Haen), Acetic acid glacial (Analar Norma-

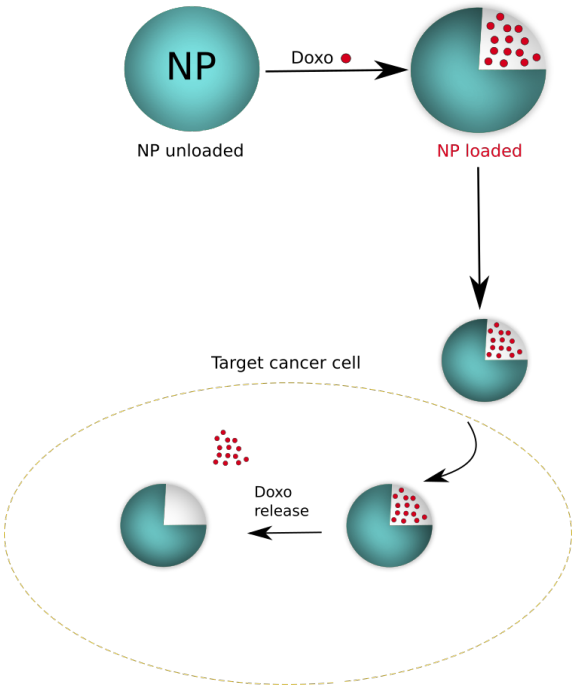

Figure 6.1: Scheme DOXO cell release

pur), mercaptosuccinic acid (Sigma Aldrich), dialysis sacks MWCO 1200 Da (Sigma Aldrich), Sodium Chloride (NaCl, Panreac), Sodium hydroxide (NaOH, EKA), Hydrochloric acid (HCl, Panreac), Phosphate Buffered Saline (PBS, Amresco), DOXO hydrochloride (DOXO, Sigma Aldrich), Dimethyl Sulfoxide (DMSO), Modified Eagle's Medium (DMEM), ethanol, fetal bovine serum (FBS), thiazolyl blue tetrazolium bromide (MTT). Measurements were realized in UV-vis spectrophotometer Evolution 220 from Thermo Scientific., F-4500 fluorescence spectrophotometer (Hitachi, Japan).

6.2.2 Preparation of Apo

Apo was prepared using, previuosly procedure, described in reference [65], with minor modifications. The ferritin equine spleen Type I (224 μl, 0.34 mmol) was diluted until 5 mL 0.1 M $NaOAc$ buffer (pH 5.5). First, was dialyzed against 152 ml of $NaOAc$ buffer (0.1 M) at pH 5.5 for 20 min. Then, was added to the ferritin solution mercaptosuccinic acid (371 μl, 0.1 M) and dialyzed for 2 h against $NaOAc$ buffer (0.1 M). Later, mercaptosuccinic acid (185 μl, 0.1 M) was added and dialysis continued for 1 h against $NaOAc$ buffer (0.1 M). Afterward, the buffer was refreshed and dialysis was

maintained for 20 min. This process was repeated until reaching a complete decoloration of the ferritin solution.

6.2.3 DOXO encapsulation

Apo-Doxo were constructed by disassembly/reassembly method reported in reference [63]. Apo solution at 0.5 mg/ml prepared with NaCl (16 μl in 5 ml of NaCl) was adjusted to pH 2.0 by addition of HCl (0.1 M) and incubated for 10 min. DOXO (0.01 mg/ml) was added to the solution and the pH was maintained for 5 min. Then, the pH was increased to 8.0 using NaOH and was stirred at room temperature for 30 min. The resulting solution was dialyzed against PBS to remove inbound DOXO for 2 h. After dialysis, solutions were centrifuged at 3500 rpm for 40 min at 4°C and supernatant was collected.

6.2.4 Intrinsic emission fluorescence

The fluorescence spectra of Apo-Doxo and Doxo standard were analyzed using fluorescence spectrophotometer. Spectra were recorded on a 1 cm path-length cuvette with an excitation slit width of 20 nm and an emission slit width of 20 nm. The excitation wavelength was set at 480 nm and the emission spectra were recorded at 500 nm to 700 nm.

6.2.5 Cell culture

Human breast carcinoma cells (MCF-7) were culture in Dulbecco's Modified Eagle Medium (DMEM) (Sigma, PT), supplemented with 10% Fetal Bovine Serum (FBS, Invitrogen Life technologies, UK), 1% penicillin/streptomycin (Invitrogen Life technologies, UK) and 3,7 g/L sodium bicarbonate and maintained at 37°C in a humidified atmosphere containing 5% CO_2. The cells were used between passages 17 to 29.

6.2.6 MTT viability Test

MCF7 were seeded in a 96-well plate at a density of 1x105 cells/well and incubated in complete medium at 37°C for 24h. Treatment was administered after 24h. DOXO was formulated into concentrations of 0, 0.05, 0.1, 0.2, 0.4, 0.8, 1, 1.6 and 3 μg/ml, and 3 replicate wells were used for each concentration, with a final volume of 200 μl. NP loaded with DOXO was add in triplicated and Apo was used as control of NP not loaded. Following 24h of treatment incubation washed with PBS and starting the MTT measurements, added

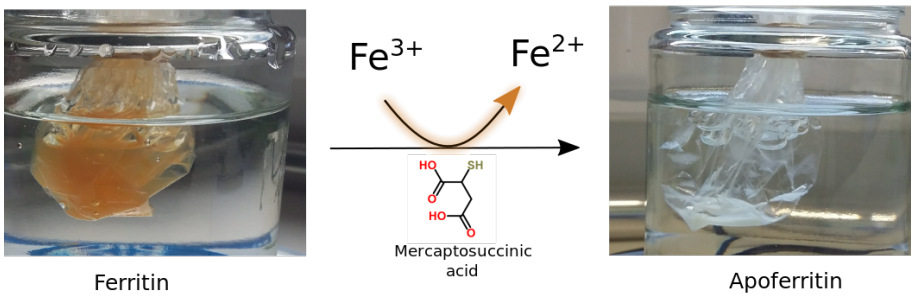

Figure 6.2: Scheme for Apo preparation

20 μL of 20 mM MTT (dissolved in PBS). After incubate the cells for 3 hours at 37°C, the MTT solution was carefully removed and 200 μL DMSO was added in order to solubilize the violet formazan crystals. The plates were then shaken on a horizontal shaker for 15 min to allow for complete dissolution. The optical density (OD) was read using a spectrophotometric microtiter plate reader set at a dual wavelength of 550/650 nm.

6.3 Results

Figure 6.2 show that the iron core is extracted. The transparency of the ferritin protein in solution evidence the absence of the iron core. In this manner we obtained the apoferritin nanoparticle prepared for loaded a DOXO.

The empty iron cavities of Apo nanocages are used for DOXO encapsulation by a reassemble route involving pH variations. The Transmission electronic microscopy (TEM) images indicated the similar morphology and size of Apo-Doxo and Apo. The corresponding TEM image confirmed the formation of the expected protein nanocages (see fig: 6.3).

Intrinsic fluorescence of DOXO can provide information about its concentration and biodistribution. This fluorescence is an important tool to confirm that the vehicles has DOXO inside (fig: 6.4).

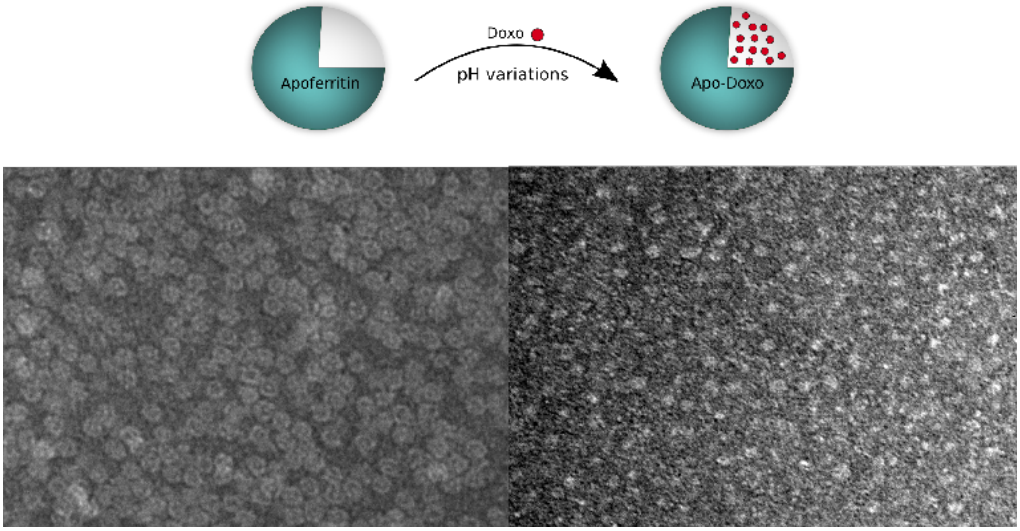

Figure 6.3: SEM image: left for Apo and right for Apo-Doxo.

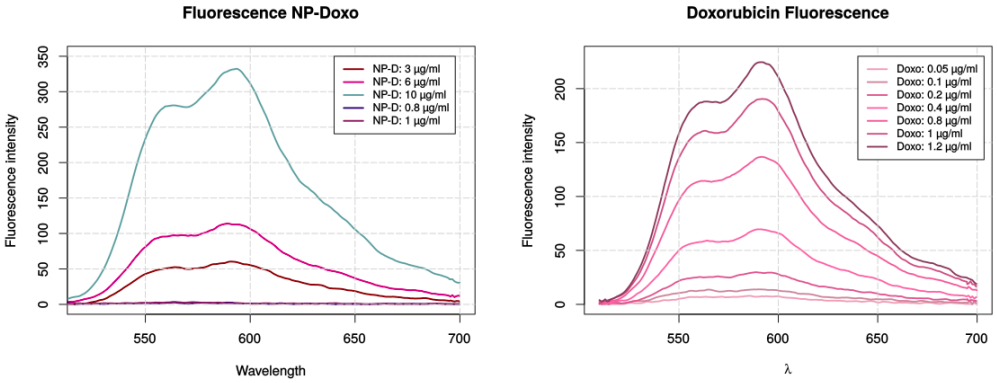

Figure 6.4: Fluorescence spectra: left differents Apo-Doxo concentration and right calibration curve for Doxo.

According to the FDA, IC50 represents the concentration of a drug that is required for 50% inhibition in vitro, see Table:6.1.

DOXO μg/ml	OD value	IR (%)
0	0.703^{+}_{-} 0.04	0
0.05	0.688^{+}_{-} 0.05	2.13
0.1	0.655^{+}_{-} 0.05	5.45
0.2	0.636^{+}_{-} 0.03	9.53
0.4	0.539^{+}_{-} 0.03	23.32
0.8	0.363^{+}_{-} 0.08	48.36
1.6	0.104^{+}_{-} 0.07	85.16
3	0.128^{+}_{-} 0.003	81.69

Table 6.1: Table for Inhibitory rate for DOXO

The inhibition of cell growth (IR) was calculated using the following equation:

$$IR(\%) = (1 - \frac{OD_g}{OD_c}) * 100 \tag{6.1}$$

where:

- R: Inhibitory rate (%)
- OD_g = mean OD value in the experimental group.
- OD_c = mean OD value in the control group.

Cell viability assay was through the MTT. MTT reagent is added to the medium and to incubate between 1 to 4 hours. When we performed this protocol in 24 and 12 hours treatment, the results were incongruous, we obtained more metabolic activity in higher concentrations that were against all previous published results.

We hypothesize, that the results were due to DOXO coloration and a possible interaction with the pH indicator of the medium, in this case, phenol red. Taking this in account, we decided to performed several washes before and do the incubation with MTT reagent with PBS. It was finally obtained the expected curve where is possible to obtained the IC50 value, fig: 6.5.

Was realized the MTT assay in MCF7 cell line for NP loaded with two DOXO concentration: 0.8 and 1 μg/ml, and DOXO: with same concentration and NP only as control. The cell viability in MCF7 cell line after evaluated by the MTT assay for DOXO is shown in fig: 6.6. The aim for this assay was the DOXO maintained its pharmacological activity.

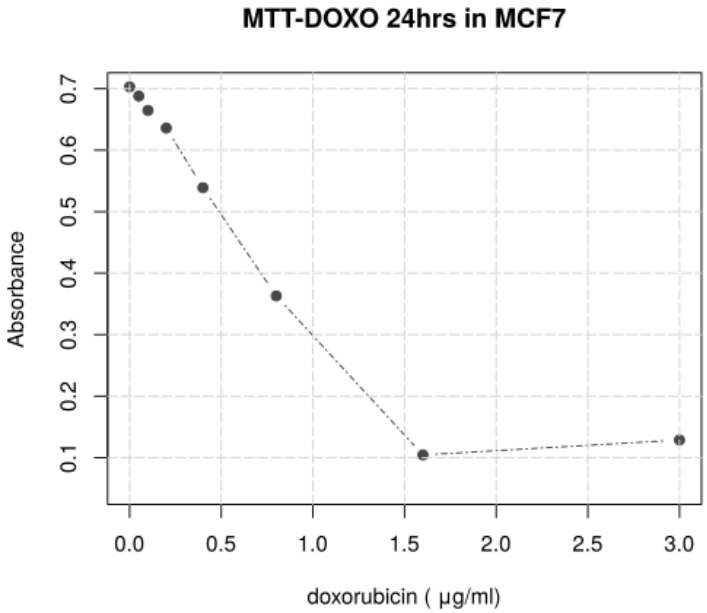

Figure 6.5: MTT assay for Doxo at 24 hrs.

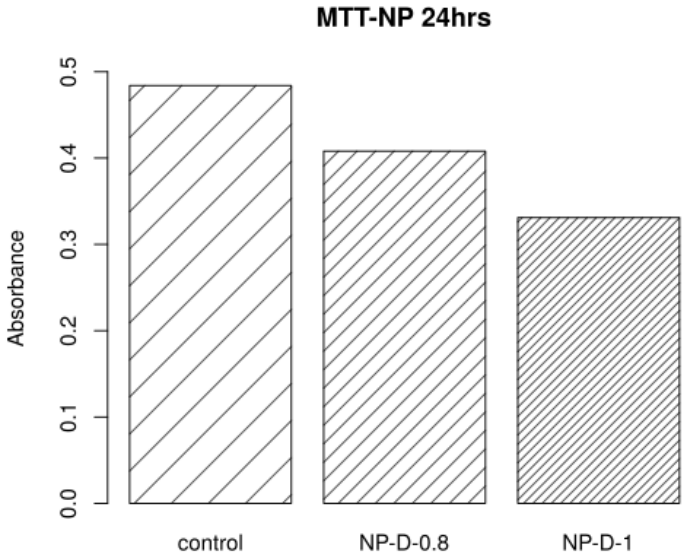

Figure 6.6: MTT assay at 24 hrs.

6.4 Discussion

Iron storage protein ferritin, as a template for Apo-DOXO preparation. DOXO fluorescence is dependent of several variables, mainly if DOXO is conjugated with other biological compounds, with proteins and membrane systems exhibit variable effects on DOXO fluorescence. One way to understand the potential effects of the interaction with model cellular compounds was to compare the fluorescence spectra of the final compound with the characteristic spectra obtained from DOXO fluorescence. The fluorescence spectra standard and Apo similar indicated, the structural integrity was not affected by the encapsulation procedure. Using DOXO as a single form of treatment, we could conclude that the most efficient concentration 0,8 μg/mL, IC50 value (half maximal inhibitory concentration).

MCF-7 cell used in many application as model to investigate the application in antitumour drugs. In this study, it was shown that the encapsulated DOXO has an antiproliferative effect in MCF-7. This confirmed the reported, in the literature [66,67], that loading ferritin with DOXO is successful strategies, and particularly their release into the cell.

6.5 Conclusions

In conclusion, we have prepared Apo from ferritin and we exploited a properties of reassembly of Apo nanoparticle to incorporate DOXO. Our work present an efficient method for the encapsulation of DOXO, confirmed the characteristic fluorescence spectra of DOXO that were not modified as a consequence of the encapsulation. The pharmacological properties of DOXO as chemotherapies in treatments cancer continue, to be effective against MCF-7 cells.

7 Conclusions

In this report, I have reviewed my professional path as biochemist. I finished my Biochemistry degree in 2010. During this period I learned about ischemia process and I gained skilled in many laboratory techniques, such as spectrophotometer, animal surgery and behavioral trials. Work in something that could lead to a better understanding about how ischemia happens, and how it can be treated. The purpose of this study was to describe alterations in oxidative metabolism in the cortex, striatum, and hippocampus, and the effect of these changes on memory, and learning disorders in a rat model of cerebral hypoperfusion. One of the things I liked more at this time was the fact that this may potentially have an impact in real lives.

After obtaining my degree, I started as junior researcher in September 2010 at IPK institute, Havana, Cuba. Here I was involved in a study to identify NoV by RT-PCR, to know the clinical characteristics and association with RoV infection in children aged less than five years. I learned HIV microelisa, detection of HBsAg, ELISA, SDS-PAGE, DNA and RNA extraction, RT-PCR, Real-Time PCR, immunofluorescence, agarose gel electrophoresis and cell culture.

Later in Portugal I continued my research career at INESC-TEC developing a biosensor for bacterial detection. We used *B. thuringiensis* strains as model of *B. cereus* in the construction of electrodes. The goal was to built a sensor for bacteria/spore recognition, using the molecular imprinted technique. In this opportunity, I learned how the development of biosensors can have an impact in the early detection of outbreaks, and about how can they prevent its propagation. I gained skill in electrode construction.

Finally, I'm currently working at BioMark in Porto, Portugal, and my current investigation is to develop a apoferritin nanoparticle loaded with DOXO. This is an interesting approach in the sense that Trastuzumab will

be used not only as a drug but also as the smart delivery targeting system. We continue working in this direction for obtained an effective system for smart drug delivery. Until now, I learned more about cell culture, electrochemical measurements, building of immunosensor, breast cancer and nanomaterials.

Appendix

A

Shiga Toxin Detection : A Short Review

Shiga toxin is secreted by certain types of bacteria, like Shigella dysenteriae and certain strains of Escherichia coli bacterias. Shiga toxin and the closely related Shiga-like toxins represent a group of very similar of cytotoxins that may play an important role in diarrheal diseases and in the hemolytic-uremic syndrome. The outbreaks caused by this toxin create serious public health crisis with significant economical cost. In the past years there has been research relative to finding specific protective measures or therapy against the infections provoked by STEC. The supportive therapy, which includes antibiotics or antidiarrheals, may potentially lead to more severe manifestations of the disease, as some recent clinical result have shown, thus looking for alternatives approaches is required. On the other hand, the knowledge of the molecular structure of the toxin will provide useful information that may be used in therapies and vaccine candidates for certain types of cancer and infectious diseases. At the present are necessary techniques of rapid identification, simple and sensitive which can be employed in the countryside with minimally-sophisticated instrumentation. Biosensors have shown tremendous promise to overcome these limitations and are being aggressively studied to provide rapid, reliable and sensitive detection platforms for such applications.

A.1 Introduction

A.1.1 Preliminaries

Shiga toxin was discovered by Kiyoshi Shiga in 1898, and named it Bacillus dysenterie [68]. In his work, Shiga described the production of the toxic factors actually known as Shiga toxin [69]. Shiga toxin-producing Escherichia

coli (STEC) was discovered in 1977, and it was associated with the clinical hemolytic-uremic syndrome (HUS) in 1983, a life-threatening condition characterized by hemolytic anemia, thrombocytopenia, and renal failure [70]. This toxin has been also associated with hemorrhagic colitis and other severe disease conditions. Most of the work in the identification and characterization of Shiga toxin has been focused on E. coli O157:H7 strains, although many cases of Shiga toxin associated disease were caused by other serotypes of E. coli [68].

The main reservoirs of STEC are cattle and sheep, but other animals are recognized as a risk factor such as deer, dogs, birds and horses. Nevertheless, new vehicles of infection as an enviromental contamination and the intensive farming are continuously been identified [71]. Shiga toxin-producing Escherichia coli may cause diarrhea, bloody diarrhea and hemorrhagic colitis. The transmission of STEC may occurs through contaminated foods, such as ground beef, through contaminated water and by person-to-person interaction [72]. Fecal-oral transmission is also a common mode of transmission. Other ways to acquire that disease is the ingestion of contaminated food or direct contact with animals on farms or at zoos. The leafy greens and unpasteurized apple cider are other recognized exposure sources. The transmission from person-to-person can occur directly (households, child care centers, institutions) or indirectly (contaminated drinking or recreational water). The ingestion of undercooked hamburgers in fast-food restaurants, was associate with the production of hemorrhagic colitis (HC), produced by STEC. Stool cultures from patients infected in these episode, yielded a previously rarely isolated E. coli serotype, $O157 : H7$. It has been reported that many E. coli strains isolated from these inpatients with diarrheal illness produce a Shiga-like toxin (SLT), including one of the strains that produce the Vero cytotoxin [73] Afterward O'Brien et al., showed that Shiga-like toxin and the Vero cytotoxin were the same toxin [74] Bacterial infections caused by Shiga toxin are responsible of many disease and the death of a great number of people. These infections have become a growing threat to the human health with worse manifestations in developed countries where the bacterias able to release Shiga-like toxins has been found in different food, including milk, apple juice and vegetables [75].

Surveillance data from the Center for Disease Control (CDC) of the U.S. for the 1998 calendar year showed an increase in the number of confirmed outbreaks of E. coli $O157 : H7$ infection, from an average of 31 per year between 1994 and 1997 to 42 in 1998. In most of the Asian countries, STEC is not yet a major health problem, except in Japan, where 29 outbreaks were reported between 1991 to 1995 [74]. The first documentation of outbreak produced by strain $O157 : H7$ was in 1982 causing hemorrhagic colitis.

Since then, the incidence of this strain in the diseases has increased annually [76]. An important massive outbreak of $O157 : H7$ that gained particular attention happened in the western U.S. in 1993, having 501 cases, 151 hospitalizations and 45 cases of HUS. This outbreak was linked to consumption of undercooked hamburger meat at a fast food restaurants [77]. More recently, the transmission of foodborne bacteria remains an important public health threat because of the increased consumption of fresh vegetables and fruits, and the increased consumption of foods in public restaurants. The 80%of cases of bacterial diarrhea that occurs every year in the United States are a result of foodborne transmission. Shiga toxin–producing E. coli is among the four most commonly reported bacterial enteropathogens and contributes to an estimated cost of $7 billion annually. STEC in particular, causes approximately 100,000 illnesses, 3,000 hospitalizations and 90 deaths annually in the United States [78].

Numerous outbreaks, as well as sporadic cases of STEC infections and HUS, have been documented worldwide. The largest outbreaks were recorded in industrialized countries. The modern industrialized large-scale food production might serve as a widespread vector in cases of food contamination. In Germany, STEC were commonly recognized as pathogens causing rare but severe disease almost exclusively in younger children. Before 2011, about 1,000 STEC infections per year and fewer than 100 cases of HUS were registered. The 2011 outbreak of a STEC $O104 : H4$ in Northern Germany started at the beginning of May, reaching its peak on May 22. This an unusual outbreak of diarrhea with HUS affected Germany and was spread to other European countries, United States and Canada. Until July 4, when the end of the outbreak was officially declared 4075 cases: 3935 in Germany, with 48 dead, while in set of the other countries affected during this outbreak, were reported 140 cases [79].

The most comparable historical outbreak to the recent German epidemic, was took place in Japan in 1996 (Sakai city outbreak). About 6,000 persons were affected after white radish sprouts had been served at school canteens, exposing 47,000 children to the contaminated food. The incidence of HUS in the Sakai city outbreak was considerably lower (106 cases out of 6,000 infections). Another outbreak of a STEC $O157 : H7$ have occurred in 1996, in Scotland, involving 512 persons, of whom 279 cases were microbiologically confirmed. One of the largest non-O157 STEC outbreaks was caused in Oklahoma in 2008, which reported 341 cases with gastroenteritis, 71 patients required hospitalization and 1 patient died [80].

The virulence of E. coli 0157 : $H7$ can partially be attributed to its ability to establish infection at low doses in humans. The majority of STEC infections present with hemorrhagic colitis as 91% of patients give a history

of bloody diarrhea at some point during their illness. Significant morbidity and mortality secondary to infection is attributed to the development of HUS [78]. Among the E. coli $O157 : H7$ has received the most attention by the scientific and regulatory community because of its association with several large outbreaks of human illness with severe manifestations. Even when the growing knowledge about toxins and its interaction with cells have allowed the production of molecules that help to treat this type of infection [75], this help some times comes out of time, as most of the above infections where confirmed several days after the initial episode.

The knowledge of the functions and the molecular characterizations of Shiga toxin have helped in possible disease intervention strategies as well as exploitation of the toxin in cancer therapy and immunotherapy have been explored. It is known that available methods are not characterized by its speed. However, it is our intuition that biochemically-driven toxin detection can improve the speed of diagnosis kits for bacterial diseases. Currently, no extensive research on Stx identification and quantification is available. The purpose of this work is to review the state-of-the art techniques for Stx detection, trying to describe all the biological and (bio)chemical approaches for its diagnostics.

A.2 The Shiga family of toxins

A.2.1 Structural Characteristics

Shiga Toxin and Shiga-like Toxin belong to large family of plants and bacterial toxins. The real Shiga Toxin (Stx) is produced by Shigella dysenteriae and is almost identical to Shiga-like toxin 1 (Stx1). Shiga-like toxin is secreted by some strains of Escherichia coli (STEC), and also Citrobacter freundii, Aeromonas hidrofilas, Aeromonas caviae y Enterobacter cloacae have been reported able to express the toxin. Although the Shiga-like toxin is have a similar structure, do not have the same effect on cells [81]. The family of Shiga toxins is referred as Stxs, when we mentioned to Shiga toxin is the protein produced by S. dysenteriae , while that the two forms produced by STEC are named Shiga toxin 1 (Stx1) and Shiga toxin 2 (Stx2).

As said before, the virulence factor of Shiga toxin, also known as verotoxin, causes hemorrhagic colitis and diarrhea and in the most severe cases leads to the lethal hemolytic-uremic syndrome. The primary virulence factor in systemic host responses produced by clinical isolates of STEC is Stx2, but some isolates produce both Stx1 and Stx2, or more rarely only Stx1 [82].

The two serological types of verotoxin, Stx1 and Stx2, are formed by a

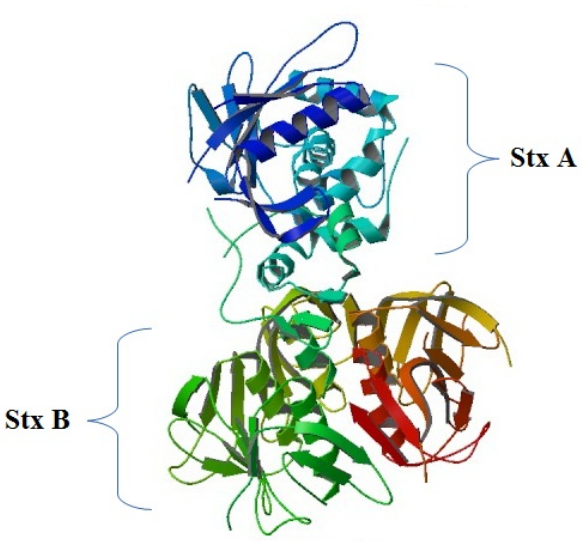

Figure A.1: Is shown the subunit A and B of Shiga toxin. (Taken from RCSB Protein Data Bank)

active enzymatic complex with a subunit A and five subunit B (Figure A.1) [46]. The molecular weight of the toxin is around 70kD, composed by subunit A of 32 kD and each subunit B of 7.7 kD . The disulphide bonded loop near the C-terminal of the A subunit is formed by two cysteines (between Cys242 and Cys261). This internal disulfide bond is proteolytically processed by furin that recognize of specific sequence motif ($Arg-Val-Ala-Arg$), generated two subunit: A1 ($28kD$) and A2 ($4kD$). Not only the sequence known to be a furin-recognition site is required for efficient cleavage, but also the amino acids structure around this site are important for furin processing [**?**]. The A1 fragment possesses a highly specific RNA N-glycosidase activity, it inhibits protein synthesis after it is released in the cytosol by the elimination of adenine at position 4324 from the 28S RNA of the 60S ribosomal subunit [83]. The B pentamer, of 89 aminoacids, can join the terminal of disaccharide galabiose ($gal-\alpha 1,4-gal$) in the surface of the host cells. This interaction carbohydrate-toxin can be used to STEC detection [84].

Stx1 is virtually identical to Stx, differing in only one aminoacid residue in the A moiety, whereas the Stx2 isoforms share less sequence similarity with Stx (60%), and cannot be neutralized by antibodies against either Stx or Stx1 [85]. Toxins Stx1 and Stx2 have similar structure but differ in their sequences (Figure A.2): the fragment A has 315 aminoacid, while for Stx2 the subunit A show 318 aminoacid [75]. Although their primary sequence of aminoacid are related, Stx1 and Stx2 are immunologically different: both

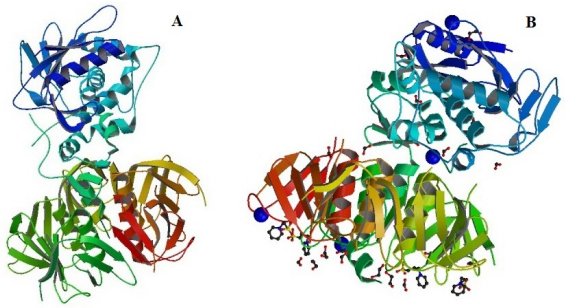

Figure A.2: In the fig 2A is shown the Stx1 and in the fig 2B Stx2. (Taken from RCSB Protein Data Bank)

are able to join the Gb3 receptor but they do not target same organs and tissues. [86].

A.2.2 Genetics Encoding

The Shiga toxin genes are located in the bacteriophage lambdoid (bacteria virus), which is associated with all pathogenic STEC. These genetic elements play an important part in horizontal gene transfer and the genome diversity. The Stx genes are highly expressed when is activated the lytic cycle of phage. The production of toxins is regulated through of some mechanisms as: the phage gene promoters, the toxin liberation and the amplification of gene copy number [87]. For ease transport to periplasm of the protein, both the A and B subunit, are expressed with N-terminal signal peptides. It are removed in the mature protein when is released from the bacteria.

The different variants of Shiga toxin are produced due to the bacterial host cells are capable of carrying many Stx-phages. These multiple Stx-phages are genetic entities with characteristic that influence in toxin production and thus virulence of the host bacteria [87].

A.2.3 Shiga Receptor

The ability of the Shiga protein for binding to carbohydrates with terminal $(gal - \alpha 1,4 - gal)$was exploited as purification systems of all toxin variants and the B subunit. In the eukaryotic cells the surface receptor for members of the Stx family is the neutral glycosphingolipid globotriaosylceramide ($Gb3$), with exception of Stxe variant that recognizes the globotetraosylceramide ($Gb4$) Glc-ceramide. Several synthetic analogues of Gb3 that could distinguish between Stx variants, with a modification in the N-acetyl group.

Many sites of binding to Stx are available, due to that each the subunits in the B pentamer have three sites of Gb3 binding [88].

Gb3 is expressed in many cells of the body human, but the fact that between the more common complication are hemorragic colitis and the HUS, suggests that the infection is directed to specific organs. For example, Gb3 is expressed in the kidneys fundamentally in the pediatric glomeruli, and when the kidneys become in adult this expression decreases or loses. This explains because the HUS occurs mainly in children caused by Stx1 [89]. Has been reported that in the 90% of HUS cases is occurs in children less than 3 years. Furthermore has been observed that the Stx1 is binds little or nothing in adults renal glomeruli [90].

The affinity of Stx1 by the receptor Gb3 is ten times bigger than it with Stx2. The Stx1 and Stx2 are secreted of different ways and are different translation across the outer membrane [**?**]. Gb3 is synthesized in the Golgi of eukaryotic cells and is transported to the plasma membrane, having its trisaccharide residue out and the non covalent ceramide hydrocarbon in the plasma membrane. The subunit of joint of Stx specifically recognizes the terminal alpha 1,4 trisaccharide digalactose. Not only the part of carbohydrate is important in the toxin join but also the lipid tail is important in the interaction of toxin with its receptor. The sensitivity of the cell to the toxin and the joint between the toxin and the cell can be regulated by many factors which induced the production of new receptors for the Shiga toxin. The increased in many types of cell of the Gb3 production carries a high effectivity the infection process [75].

A.2.4 Mechanism of action

It is well known that all subunits of Shiga toxins are essential in the infection process of cells target. The B subunit is responsable for the binding at cell receptor and the A subunit for the inhibiting of protein synthesis [86].

The induction of Gb3 production is the mechanism that facilitated the action of Shiga toxin and the severe complication during the infection. The internalization of toxin involves formation of a clathrin-coated pit on the cell membrane. The toxin is degraded in the fusion process with the lysosome cellular. In cells that are sensible to Stx, the endosomal vesicle contain a complex receptor of toxin submitted to a retrograde transport way Golgi to endoplasmatic reticule. In the lysosoma the protease of membrane furin-like cleaved the subunit A, generating a catalytically active A1 N-terminal fragment and a A2 C-terminal fragment that remain attached by a disulphide bound. The active catalytically fragment exerts its effect upon the ribosomes when is realeased in the cytoplasm, provoking a rapid intoxication and the

cell death [81, 91].

Shiga toxins are potent ribosome-modifying enzymes, but it not limited its action in the inhibition of protein synthesis. They have cellular effects, including the induction of cytokine expression by macrophages [87]. The toxin induce a serie of chain reaction through the release of many factors facilitating the proteolytic attack and DNA degradation [75]. Toxin can exerts its effect in eukaryotic cells and the end result of this event is the programmed cellular death or apoptosis and contribute at the rapid intoxication a level of organism [86]. The basic knowledge about the toxins, its mechanism of action and interaction mode a molecular level, is fundamental to guide the researches toward construction of molecules for used in therapeutic or diagnostic methods and guarantee the control of diseases. The protein toxins have been used in studies for understand the endocytic process and intracellular transport in general. Shiga toxin studies were the first in show that a molecule can be translocated from cellular surface through of cellular organelles [75].

A.3 Medical Applications

Shiga toxin is associated with epidemic outbreaks every years, but its toxic properties have been used for medical purposes. In the cancer cells the glycosphingolipid composition and metabolism suffer dramatic changes. These changes provoke alteration in the ability of glycosphingolipid to bind the antibody and induced immune response in the tumor cells [92]. It is known that many cancer cells is Gb3 overexpress, which is an advantage for use of Stx as therapy methods and target for kill tumoral cells [85]. Stx is efficient in killing cancer cells due to is capability to arrive the cytosol. In many research has been shown how the Shiga holotoxin inhibits the tumor growth in mouse models. The Shiga B moiety is used like vehicle transport of conventional cancer drugs directed to Gb3-expressing cells [93]. The use of Stx B as vector for peptide delivery to the MHC class I pathway for the development of vaccines is favoured because the limited expression of Gb3 receptor in normal human cells. Some brain tumor cells are sensitive to Stx1 and are killed by apoptosis process. The toxin have been related with the ability to metastasize in colon cancer cells and has been suggested the idea of using Stx for the diagnosis of cancer cells. This has been tested in murine models with obtaining positive results [75].

The treatments of Shiga toxin infection with antibiotic are controversial because can be increased the progression to HUS in patients. There are evidence that patients treated with antibiotic therapy had a than 50 % chance of HUS develop, whereas that those not treated only an 8 % of possibility

to progress to HUS. Studies of potential treatments are ongoing due to the antimicrobial treatment is risky. Actually, the strategies are focused in find the mechanism of rapid detection for this toxin causing bacterial outbreaks every years [94].

The cross-neutralization has been achieved in animals vaccinated with chemical prepared of Shiga toxoids, but the use of these chemical Stx toxoids in human is potencially toxic. Therefore, have been develop genetic toxoids through of specific mutation in the A subunit of Stx that permit its use in human treatment. There are studies that show the Shiga toxin is a promising vaccine candidate. For example, has been determined that the immunization with genetic toxoides of Stx1 and Stx2 is protective against heterologous toxin in animals models. In other work, is used plant-based vaccine to Stx2 toxoid to protect against systemic Stx2 intoxication. The monoclonal antibodies against Stx1 and Stx2 shown positive results for their use as tools in the STEC diagnosis and therapy [85].

A.4 Detection

A.4.1 Biological Methods

It is considered that an appropriate response to bacterial outbreaks consist in its early detection and the use of adequate antibiotics to control them. The methods used to detect food pathogens have been grouped in four mainly categories. In the first group are the conventional microbiological methods, in which the food is mixed with selective medium enriched to increase the population of a target organism. Also, in this categories is located the agar plating in selective or differential media to isolate the pure culture, and the test of the culture by means of phenotype analysis or take of metabolic fingerprinting. These conventional microbiological methods, which are considered the gold standard, are reliable and accurate, but require much time and are very labor intensive to obtain the results [95]. Typically, the traditional methods involve a series of steps: pre-enrichment, selective enrichment, biochemical screening and serological confirmation. These step are laborious, requiring significant amount of time, expensive equipment and trained personal [46].

The detection of microorganisms which produce Stx has been difficult, due to the microorganism diversity and the detection limits of the samples in the environment [76]. The bacterial detection methods have to be rapid and very sensitive since the presence of even a single pathogenic organism in the body or food may become infectious. Extremely selective detection methodology is required, due to the big numbers of non-pathogenic organisms, which

are often present in a complex biological environment, and coexist with the pathogenic bacterias. The traditional methods used for identification of bacteria comprises the counting of cells with the aid of a optical microscope or by flow cytometry; measuring physical parameters by piezocrystals, impedimetry, redox reactions, optical methods, calorimetry, ultrasound techniques and detecting cellular compounds such as ATP, DNA, protein, lipid derivatives and radioactive isotopes [45].

The second group is composed by variants of the polymerase chain reaction (PCR) technique. Numerous articles has been published employing these methods in the determination of pathogens amongst them, E.coli in food. The methods to detect and identified the verotoxin produced by E.coli, based in these PCR genetic techniques, have been developed very recently. An advantage of this techniques is that with small amounts of samples make possible the accurate detection of the target species [96]. The PCR technique is very sensible for this task, but require hours to process the sample. Besides considerable bio-molecular skills are needed to prove the identification. The whole process could take from 48 hours until five days in obtain the result, moreover of the delay in the transportation of sample to the lab [97]. Moreover, the presence of certain genes has not, necessarily, a direct correlation with dangerous toxin levels [46].

The PCR in real time is the most used to the quantification of specific fragments of DNA. The amount of product synthesized during PCR is measured in real time by the detection of a fluorescent signal produced to result of a specific amplification. This methods is rapid and sensitive, but in some cases show false positive and negative results, requiring an additional confirmation through to the hybridization probe and polymorphism of length of restriction fragment [95]. Several methods based in the PCR in real time have been commercialized to the analysis of Shiga toxin genes in microbiologic food [98].

The third group includes the methods of immunosorbent assay (ELISA), its principle is based in the join of an antibody to the target antigen. It is a method accurate and precise, ideal for the quantitative and qualitative detection of many types of protein in complex matrices when the objectives are known. The sensitivity is low and it is necessary up to 3 or 4 hours to complete the analysis [95]. The ELISA for Stx1 and Stx2 can be used in stool sample. There are also commercial immunoassay for the detection of the Shiga-like toxin in milk and chopped meat [99, 100].

One of detection methods based in the capture of antibodies was realized by Hattum et al. The presence of verotoxin in the sample is obtained through a fluorescence signal coming of antibody anti-biotin. The method is complementary to genetic methods, because allow the detection of mRNA but not

provides information about if the toxin is expressed or if it is functional [46].

The researcher Ashkenazi et al, have evaluated the efficacy of a Gb3-based ELISA for detection of Shiga toxin, both from culture pure plates and, most importantly, directly from a mixed bacterial culture [101].

The glycodendrimers and glycol-conjugated nanoparticles has been used as anti-adhesive molecules for toxins and biosensors to monitor the protein-carbohydrate interactions. The glyconanoparticles show the best potential for studying these protein-carbohydrate interactions. The size distribution of these nanoparticles is reasonably narrow and is comparable with the size of the studied biomolecules, are fine described and are easily manipulated chemical structures. The glycopolydiacetylene nanoparticle (GPDA) has been used to monitor receptor-ligand events junctions for viruses, toxins, bacteria and antibody-receptor interactions, due to its unique colorimetric transition when joining to these macromolecules. Therefore, due to the well-known affinity of Shiga toxin towards the final $[gal - \alpha 1, 4 - gal]$ disaccharide unit, GPDA nanoparticles containing this specific disaccharide sequence has been used to identify E.coli Shiga toxin in in 96-well plates [84].

The fourth, and most recent group of detection is based on microarray techniques. These methods allow the simultaneous identification, in the foods, of a large number of pathogens with a simple reaction. The basic idea is that many probes selected are joined in a matrix shape on a solid surface, each one of these site contains several copies of specific probes. The matrix is hybridized with the DNA isolated from the sample of interest, producing a characteristic fluorescence. During this step of hybridization, the fragment is joined to the probe about the bases of DNA complementarity. However, the methods of regular microarrays needed expensive equipment for exploring that matrix and recopilaing the generated data [95].

A.4.2 Detection by Biosensors

Many of the reported methods for the detection of pathogenic bacteria are applied to Escherichia coli. Most E.coli-specific methods have a detection limit between $10^3 and 10^5 cells/mL$ and some rely on the amplification of specific genes of the E. coli genome for specific identification [102]. The biosensors have been recently considered as attractive alternative to conventional platforms for pathogens detection. Moreover, biosensors does not lack of desired characteristics, such as high grade of sensitivity and detection specificity, minimum effort in sample preparation, profitability, miniaturization and portability to real-time monitoring while reduce the total time requested for detection. Therefore, a great effort has been allocated the development of rapid biosensors of diverse nature, as they are considered promising devices

for pathogenic bacteria detection [103].

Ideal attributes of any element of recognition would be a great stability, facility of immobilization in the sensor platform and the specificity of recognition to the host with minimal cross-reactivity to other pathogens agents [104]. In the detection of biochemical and physiological processes, the biosensors have been converted in a fundamental tool.

Acording to the methods used for signal transduction, biosensors are divided in four groups: mass, optical, electrochemical, and thermal sensors. taking into account the way used for target identification, biosensors can be classified into two categories: sensors for direct detection and sensors with indirect detection. Direct detection biosensors are designed in such a way that the biospecific reaction is directly determined in real time by measuring the physical changes induced by the complex formation. Whereas indirect detection biosensors are those in which a preliminary biochemical reaction takes place and the products of this reaction are then detected by a sensor.

Very often, they have been grouped into the following categories: biosensors based on direct detection of bacteria, flow-injection biosensors, monitoring bacterial metabolism, detection of enzyme labels, genosensors and the emerging artifical nose [45]. The most popular bio-probes that have been employed in the surface of biosensors to detection of pathogens are nucleic acid, antibody, entire phages, phage display peptide (PDP) and more recently the phage's receptor binding proteins join to phage receptors in the bacterial surface. Biosensors does not a long time of sample pre-enrichment is required nor a step of secondary enrichment, and therefore, can predict the level and type of contamination of food faster than biological, microbiological, immunological and conventional molecular methods [104].

For long time nucleic acid lateral flow immunoassays (NALFIA) has been used as biosensors for the detection of nucleic acid. In this assay, nucleic acids can be captured on the lateral flow test strips by means of relation of independent or dependent antibodies. Amongst the advantages of lateral flow strips can be mentioned: one-step, simplicity, fast results, low cost, versatile and a prolonged shelf life. Moreover if compared with traditional electrophoresis detection, NALFIA has other advantages like shorter response time and no need for hazardous reagents. NALFIA can be used how biosensor for bacterial detection due to its characteristics: test between 5 and 10 min, species selectivity, direct measurement, portable and designed for field application. This is complement with a simple manufacturing process. Finally, if NALFIA strips are used with coloured nanoparticles, an easy visual detection can be afforded. This combination overcomes the need of have expensive equipments which is a major shortcomings in the application of immunosensor techniques, a fact acknowledged by Noguera et al whom have reported

the use of a carbon nanoparticles-NALFIAs combination for rapid detection and identification of genes encoding various STEC virulence factors (vt1, vt2) [102].

The technique of Localized Surface Plasmon Resonance (LSPR) which is based in the analyzing intermolecular interactions of biomacromolecules have been used for detection of biological toxins. In the recently study developed by Nagatsuka et al, was used a portable LSPR detection system that uses glyco-chips containing Au nanoparticles coated with synthetic oligosaccharides that specifically bind toxins. The ricin, Shiga toxin, and cholera toxin were selected as the targets in this study. For every case, the LSPR detection was completed within 20 min and was highly specific to the target toxin. Because of its sensitivity, a LSPR system based on glyco-nanotechnology is competitive with other techniques and has the added advantage of being portable and for providing simple and rapid analysis in contaminated areas [105].

In an assay of rapid detection, efficient, accurate and of low cost, Sulan Bai et al have developed methods to detect pathogens transmitted by food in the surface of the optic biosensors of thin film. An advantage of this technology is that, due to the characteristic optic of the thin film to the biosensors chip, the experimental results can be visualized by the human eyes without specific instruments. Therefore, this technology avoids an initial investment on expensive instruments and can distribute to any laboratory of individual research with basic facilities for molecular biology. Generally, these methods are rapids and robust, has an excellent sensitivity and specificity, and are quite competitive its cost with existing technologies [95].

Tu et al in 2006, have developed a biosensor based on the immobilization of an antibody on a optic fiber to detect rapidly the low levels of E.coli $O157 : H7$ and toxins similar to Shiga in ground beef sample. The principle of the sensor is an type sandwich immunoassay using an antibody that is specific to E.coli $O157 : H7$ or toxins. A policlonal antibody was first immobilized on waves guides of polystyrene fiber through a reaction of biotin-streptavidin that served to entity of capture to the bacterias and the toxins. The fluorescent molecules of fiber was excited for the evanescent wave, and the portion of the emission light was transmitted by the fiber and was collected in the photo-detector at 670-710 nm [106].

Another similar approach was used by Ngundi et al in 2006, which have studied an array-based technique that provides the capability to perform multiple analysis simultaneously. They report a technique of immobilizing sugars onto planar waveguides and employing the patterned arrays to analyze carbohydrate-binding protein toxins. In this study are used an array biosensor, and are employing two monosaccharide-derivatives: N-acetylneuraminic

acid (Neu5Ac), and N-acetyl galactosamine (GalNAc) as receptors for protein toxins [107].

A.5 Conclusions

Large outbreaks of human illness with severe manifestations due to STEC in- fections have occurred in recent decades caused by Shiga toxin producers microorganisms. The high infectious capacity of these microorganism make dangerous even the presence of few individuals in a given medium, as a results these episodes has received great attention by the community scientific.

These outbreaks have taken place due to an historical little monitoring or surveillance in the food supply chain. This incomplete control on food or its precursors is attributable, in part, to the lack of standardized methods for the detection or enumeration of these bacteria in food matrices, but they are also due to the lack of consensus on which serotypes are most important. Still, other issues difficult the battle against pathogens, such as: the rapid urbanization, the increasing number of poor and hungry people around the world, the rapid development of transportation, environmental change and the human activity.

The war between humans and pathogens never ends. New diseases are con- tinuously appearing, and these organism will find more chances to interact with humans. Therefore, we must take advantage of new advances in technology and the strengthen the search to develop new diagnostic mechanisms and design new drugs to fight against infectious diseases.

In this scenario, it is a challenge to create techniques to detect the bacterias involved in these outbreaks with high degree of efficiency. In recent times, the use of structure-based designed biosensors have emerged as an alternative, with the necessary properties for reliable and effective use in routine applications. Many researchers are in the search of biosensor systems with specificity to distinguish the target bacteria in a multi-organism matrix, the sensitivity to detect bacteria directly, the adaptability to detect different analytes without sample pre-enrichment and the capacity to give real-time results. At the same time, the biosensor must have relatively simple and inexpensive configurations. In the case of Stx, little have been done in this field, no robust sensors for continuous water and food monitoring have been developed. Therefore, the necessity to explore new ways to develop robust, long-time of use sensors, exists, and its a challenge to be accomplished in the next years.

References

[1] Jeremy M. Berg, John L. Tymoczko, and Lubert Stryer. Biochemistry and human biology. *Biochemistry.*, (5th edn), W H Freeman, New York pp: 1-4., 2002.

[2] Nese Aksoy. Place and importance of biochemistry in living beings' health care and some new perspectives. *Journal of Animal Health and Behavioural Science*, Sci 2: e102., 2018.

[3] Michael Cox and David Nelson. *Lehninger Principles of Biochemistry*, volume 5, (5th edn), Barcelona. 2000.

[4] Y. Castaño Guerrero, M. E. González Fraguela, I. Fernández Verdecia, I. Horruitiner Gutiérrez, and S. Piedras Carpio. Changes in oxidative metabolism and memory and learning in an cerebral hypoperfusion model in rats. *Neurologia (Barcelona, Spain)*, 28(1):1–8, 2013.

[5] María de los Angeles Ribas, Yuselis Castaño, Marlon Daniel Martínez, Yahisel Tejero, and Yanislet Cordero. Norovirus and rotavirus infection in children aged less than five years in a paediatric hospital, havana, cuba. *The Brazilian Journal of Infectious Diseases*, 19(2):222–223, 2015.

[6] Thiruma V. Arumugam, Terry M. Phillips, Aiwu Cheng, Christopher H. Morrell, Mark P. Mattson, and Ruiqian Wan. Age and energy intake interact to modify cell stress pathways and stroke outcome. *Annals of Neurology*, 67(1):41–52, 2010.

[7] C. Arango-Davila, M. Escobar-Betancourt, G. P. Cardona-Gómez, and H. Pimienta-Jiménez. [pathophysiology of focal cerebral ischemia: fun-

damental aspects and its projection on clinical practice]. *Revista De Neurologia*, 39(2):156–165, 2004.

[8] Klas Blomgren and Henrik Hagberg. Free radicals, mitochondria, and hypoxia-ischemia in the developing brain. *Free Radical Biology & Medicine*, 40(3):388–397, 2006.

[9] A. P. Halestrap. Calcium, mitochondria and reperfusion injury: a pore way to die. *Biochemical Society Transactions*, 34:232–237, 2006.

[10] Viera Danielisová, Miroslava Némethová, Miroslav Gottlieb, and Jozef Burda. Changes of endogenous antioxidant enzymes during ischemic tolerance acquisition. *Neurochemical Research*, 30(4):559–565, 2005.

[11] D. W. Howells and G. A. Donnan. Where will the next generation of stroke treatments come from? *PLOS Medicine*, 7(3):e1000224, 2010.

[12] Eszter Farkas, Paul G. M. Luiten, and Ferenc Bari. Permanent, bilateral common carotid artery occlusion in the rat: a model for chronic cerebral hypoperfusion-related neurodegenerative diseases. *Brain Research Reviews*, 54(1):162–180, 2007.

[13] Y. Shang, J. Cheng, J. Qi, and H. Miao. Scutellaria flavonoid reduced memory dysfunction and neuronal injury caused by permanent global ischemia in rats. *Pharmacology, biochemistry, and behavior*, 82(1):67–73, 2005.

[14] CCAC - canadian council on animal care: General guidelines.

[15] S. Marklund and G. Marklund. Involvement of the superoxide anion radical in the autoxidation of pyrogallol and a convenient assay for superoxide dismutase. *European Journal of Biochemistry*, 47(3):469–474, 1974.

[16] H. Aebi. Catalase in vitro. *Methods in Enzymology*, 105:121–126, 1984.

[17] Pulok K. Mukherjee, K. F. H. Nazeer Ahamed, Venkatesan Kumar, Kakali Mukherjee, and Peter J. Houghton. Protective effect of biflavones from araucaria bidwillii hook in rat cerebral ischemia/reperfusion induced oxidative stress. *Behavioural Brain Research*, 178(2):221–228, 2007.

[18] Vesna Selakovic, Branka Petković (former Janać, and Lidija Radenovic. MK-801 effect on regional cerebral oxidative stress rate induced by

different duration of global ischemia in gerbils. *Molecular and cellular biochemistry*, 342:35–50, 2010.

[19] Tatsuo Otori, Toshiya Katsumata, Hiromi Muramatsu, Fumihiko Kashiwagi, Yasuo Katayama, and Akiro Terashi. Long-term measurement of cerebral blood flow and metabolism in a rat chronic hypoperfusion model. *Clinical and Experimental Pharmacology & Physiology*, 30(4):266–272, 2003.

[20] David S. Warner, Huaxin Sheng, and Ines Batinić-Haberle. Oxidants, antioxidants and the ischemic brain. *The Journal of Experimental Biology*, 207:3221–3231, 2004.

[21] R. Dringen, L. Kussmaul, J. M. Gutterer, J. Hirrlinger, and B. Hamprecht. The glutathione system of peroxide detoxification is less efficient in neurons than in astroglial cells. *Journal of Neurochemistry*, 72(6):2523–2530, 1999.

[22] S. Desagher, J. Glowinski, and J. Premont. Astrocytes protect neurons from hydrogen peroxide toxicity. *The Journal of Neuroscience: The Official Journal of the Society for Neuroscience*, 16(8):2553–2562, 1996.

[23] Joong-Seok Kim, Injin Yun, Young Bin Choi, Kwang-Soo Lee, and Yeong-In Kim. Ramipril protects from free radical induced white matter damage in chronic hypoperfusion in the rat. *Journal of Clinical Neuroscience: Official Journal of the Neurosurgical Society of Australasia*, 15(2):174–178, 2008.

[24] Chao Liu, Jiliang Wu, Jun Gu, Zhe Xiong, Fang Wang, Jianzhi Wang, Wei Wang, and Jianguo Chen. Baicalein improves cognitive deficits induced by chronic cerebral hypoperfusion in rats. *Pharmacology, Biochemistry, and Behavior*, 86(3):423–430, 2007.

[25] Eszter Farkas, Adám Institóris, Ferenc Domoki, András Mihály, and Ferenc Bari. The effect of pre- and posttreatment with diazoxide on the early phase of chronic cerebral hypoperfusion in the rat. *Brain Research*, 1087(1):168–174, 2006.

[26] Adam Institoris, Eszter Farkas, Sandor Berczi, Zoltan Sule, and Ferenc Bari. Effects of cyclooxygenase (COX) inhibition on memory impairment and hippocampal damage in the early period of cerebral hypoperfusion in rats. *European Journal of Pharmacology*, 574(1):29–38, 2007.

[27] Seul-Ki Kim, Kyung-Ok Cho, and Seong Yun Kim. White matter damage and hippocampal neurodegeneration induced by permanent bilateral occlusion of common carotid artery in the rat: Comparison between wistar and sprague-dawley strain. *The Korean Journal of Physiology & Pharmacology: Official Journal of the Korean Physiological Society and the Korean Society of Pharmacology*, 12(3):89–94, 2008.

[28] Rainald Schmidt-Kastner, Cristina Aguirre-Chen, Isabel Saul, Linda Yick, Duco Hamasaki, Raul Busto, and Myron D. Ginsberg. Astrocytes react to oligemia in the forebrain induced by chronic bilateral common carotid artery occlusion in rats. *Brain Research*, 1052(1):28–39, 2005.

[29] American Society of Neuroradiology. Basic neurochemistry: Molecular, cellular, and medical aspects. 7th ed. (with CD-ROM). *American Journal of Neuroradiology*, 27(2):465–466, 2006.

[30] Eszter Farkas, Adám Institóris, Ferenc Domoki, András Mihály, Paul G. M. Luiten, and Ferenc Bari. Diazoxide and dimethyl sulphoxide prevent cerebral hypoperfusion-related learning dysfunction and brain damage after carotid artery occlusion. *Brain Research*, 1008(2):252–260, 2004.

[31] Taku Sugawara, Anders Lewén, Nobuo Noshita, Yvan Gasche, and Pak H. Chan. Effects of global ischemia duration on neuronal, astroglial, oligodendroglial, and microglial reactions in the vulnerable hippocampal CA1 subregion in rats. *Journal of Neurotrauma*, 19(1):85–98, 2002.

[32] Eszter Farkas, Gergely Donka, Rob A. I. de Vos, András Mihály, Ferenc Bari, and Paul G. M. Luiten. Experimental cerebral hypoperfusion induces white matter injury and microglial activation in the rat brain. *Acta Neuropathologica*, 108(1):57–64, 2004.

[33] Erman Aytac, Hakki Oktay Seymen, Hafize Uzun, Goksel Dikmen, and Tuncay Altug. Effects of iloprost on visual evoked potentials and brain tissue oxidative stress after bilateral common carotid artery occlusion. *Prostaglandins, Leukotrienes, and Essential Fatty Acids*, 74(6):373–378, 2006.

[34] Mankin Choy, Vijeya Ganesan, David L. Thomas, John S. Thornton, Edward Proctor, Martin D. King, Louise van der Weerd, David G. Gadian, and Mark F. Lythgoe. The chronic vascular and haemodynamic

response after permanent bilateral common carotid occlusion in newborn and adult rats. *Journal of Cerebral Blood Flow and Metabolism: Official Journal of the International Society of Cerebral Blood Flow and Metabolism*, 26(8):1066–1075, 2006.

[35] Xiao-Li He, Yue-Hua Wang, Mei Gao, Xiao-Xiu Li, Tian-Tai Zhang, and Guan-Hua Du. Baicalein protects rat brain mitochondria against chronic cerebral hypoperfusion-induced oxidative damage. *Brain Research*, 1249:212–221, 2009.

[36] Evelin Vicente, Daniel Degerone, Liana Bohn, Francisco Scornavaca, Alexandre Pimentel, Marina C. Leite, Alessandra Swarowsky, Letícia Rodrigues, Patrícia Nardin, Lucia Maria Vieira de Almeida, Carmem Gottfried, Diogo Onofre Souza, Carlos Alexandre Netto, and Carlos Alberto Gonçalves. Astroglial and cognitive effects of chronic cerebral hypoperfusion in the rat. *Brain Research*, 1251:204–212, 2009.

[37] Zhi-You Cai, Yong Yan, and Ran Chen. Minocycline reduces astrocytic reactivation and neuroinflammation in the hippocampus of a vascular cognitive impairment rat model. *Neuroscience Bulletin*, 26(1):28–36, 2010.

[38] F. López, J. F. Martínez-Lage, J. Hernández-Palazón, R. López, and E. Alarcón. Actividad de la cobre-zinc superóxido dismutasa en un modelo de lesión cerebral isquémica global sin hipotensión arterial. *Neurocirugía*, 15(2):151–158, 2004.

[39] R. Prieto-Arribas, J. M. Pascual-Garvi, F. González-Llanos, and J. M. Roda. ¿cómo reparar el daño cerebral isquémico? utilidad de los modelos experimentales en la búsqueda de respuestas. *Neurología*, 26(2):65–73, 2011.

[40] Audrey Cilli, Adriana Luchs, Simone G. Morillo, Fernanda F. Costa, Rita de Cássia C. Carmona, and Maria do Carmo S. T. Timenetsky. Characterization of rotavirus and norovirus strains: a 6-year study (2004-2009). *Jornal De Pediatria*, 87(5):445–449, 2011.

[41] Shigeyuki Kojima, Tsutomu Kageyama, Shuetsu Fukushi, Fuminori B. Hoshino, Michiyo Shinohara, Kazue Uchida, Katsuro Natori, Naokazu Takeda, and Kazuhiko Katayama. Genogroup-specific PCR primers for detection of norwalk-like viruses. *Journal of Virological Methods*, 100(1):107–114, 2002.

[42] Pablo Aguiar Prieto, Orlando Rojas Martínez, and María de los A. Ribas Antúnez. Proporción de casos esporádicos de diarreas agudas causadas por rotavirus del grupo a en cuba, julio-noviembre, 2006. *Revista Cubana de Higiene y Epidemiología*, 47(2):0–0, 2009.

[43] María de los Angeles Ribas, Shigeo Nagashima, Annely Calzado, Gretel Acosta, Yahisel Tejero, Yanislet Cordero, Daynelid Piedra, and Nobumichi Kobayashi. Emergence of g9 as a predominant genotype of human rotaviruses in cuba. *Journal of Medical Virology*, 83(4):738–744, 2011.

[44] Manish M. Patel, Aron J. Hall, Jan Vinjé, and Umesh D. Parashar. Noroviruses: a comprehensive review. *Journal of Clinical Virology: The Official Publication of the Pan American Society for Clinical Virology*, 44(1):1–8, 2009.

[45] Ihab Abdel-Hamid Dmitri Ivnitski. Biosensors for detection of pathogenic bacteria. *Biosensors and Bioelectronics*, (7):599–624, 1999.

[46] Hilde van Hattum, Kim van der Zwaluw, Gerben M. Visser, Jos van Putten, Rob Ruijtenbeek, and Roland J. Pieters. Functional assay for shiga-like toxin via detection by antibody capture and multivalent galabiose binding. *Bioorganic & Medicinal Chemistry Letters*, 22(24):7448–7450, 2012.

[47] Andrew D. Dias, David M. Kingsley, and David T. Corr. Recent advances in bioprinting and applications for biosensing. *Biosensors*, 4(2):111–136, 2014.

[48] Karolien De Wael, Stijn De Belder, Sanaz Pilehvar, Geert Van Steenberge, Wouter Herrebout, and Hendrik A. Heering. Enzyme-gelatin electrochemical biosensors: Scaling down. *Biosensors*, 2(1):101–113, 2012.

[49] Manel Del Valle. Sensor arrays and electronic tongue systems. *International Journal of Electrochemistry*, 2012:e986025, 2012.

[50] Elise Cachat, Margaret Barker, Timothy D. Read, and Fergus G. Priest. A bacillus thuringiensis strain producing a polyglutamate capsule resembling that of bacillus anthracis. *FEMS Microbiology Letters*, 285(2):220–226, 2008.

[51] Patricia Buckley, Bryan Rivers, Sarah Katoski, Michael H. Kim, F. Joseph Kragl, Stacey Broomall, Michael Krepps, Evan W. Skowronski, C. Nicole Rosenzweig, Sari Paikoff, Peter Emanuel, and Henry S.

Gibbons. Genetic barcodes for improved environmental tracking of an anthrax simulant. *Applied and Environmental Microbiology*, 78(23):8272–8280, 2012.

[52] Clark Hochgraf. Using arduino to teach digital signal processing. *ASEE Northeast Section Conference 2013*, 2013.

[53] Joshua Kiepert. Creating a raspberry pi-based beowulf cluster joshua kiepert.

[54] Carol DeSantis, Jiemin Ma, Leah Bryan, and Ahmedin Jemal. Breast cancer statistics, 2013. *CA: A Cancer Journal for Clinicians*, 64(1):52–62, 2014.

[55] Mei Liu, Xiaocheng Yu, Zhu Chen, Tong Yang, Dandan Yang, Qianqian Liu, Keke Du, Bo Li, Zhifei Wang, Song Li, Yan Deng, and Nongyue He. Aptamer selection and applications for breast cancer diagnostics and therapy. *Journal of Nanobiotechnology*, 15, 2017.

[56] Mei Liu, Zhiyang Li, Jingjing Yang, Yanyun Jiang, Zhongsi Chen, Zeeshan Ali, Nongyue He, and Zhifei Wang. Cell-specific biomarkers and targeted biopharmaceuticals for breast cancer treatment. *Cell Proliferation*, 49(4):409–420, 2016.

[57] Min Yan, Maria Schwaederle, David Arguello, Sherri Z. Millis, Zoran Gatalica, and Razelle Kurzrock. HER2 expression status in diverse cancers: review of results from 37,992 patients. *Cancer Metastasis Reviews*, 34:157–164, 2015.

[58] Xiaolin Yu, Sharad Ghamande, Haitao Liu, Lu Xue, Shuhua Zhao, Wenxi Tan, Lijing Zhao, Shou-Ching Tang, Daqing Wu, Hasan Korkaya, Nita J. Maihle, and Hong Yan Liu. Targeting EGFR/HER2/HER3 with a three-in-one aptamer-siRNA chimera confers superior activity against HER2+ breast cancer. *Molecular Therapy - Nucleic Acids*, 10:317–330, 2018.

[59] Qiaoling Liu, Chen Jin, Yanyue Wang, Xiaohong Fang, Xiaobing Zhang, Zhuo Chen, and Weihong Tan. Aptamer-conjugated nanomaterials for specific cancer cell recognition and targeted cancer therapy. *NPG Asia Materials*, 6(4):e95, 2014.

[60] Kanu Chatterjee, Jianqing Zhang, Norman Honbo, and Joel S. Karliner. Doxorubicin cardiomyopathy. *Cardiology*, 115(2):155–162, 2010.

[61] Sangeeta Rivankar. An overview of doxorubicin formulations in cancer therapy. *Journal of Cancer Research and Therapeutics*, 10(4):853–858, 2014.

[62] Maria Volkova and Raymond Russell. Anthracycline cardiotoxicity: Prevalence, pathogenesis and treatment. *Current Cardiology Reviews*, 7(4):214–220, 2011.

[63] Elisabetta Falvo, Elisa Tremante, Alessandro Arcovito, Massimiliano Papi, Nadav Elad, Alberto Boffi, Veronica Morea, Giamaica Conti, Giuseppe Toffoli, Giulio Fracasso, Patrizio Giacomini, and Pierpaolo Ceci. Improved doxorubicin encapsulation and pharmacokinetics of ferritin fusion protein nanocarriers bearing proline, serine, and alanine elements. *Biomacromolecules*, 17(2):514–522, 2016.

[64] Qi Wang, Chun Zhang, Liping Liu, Zenglan Li, Fangxia Guo, Xiunan Li, Jian Luo, Dawei Zhao, Yongdong Liu, and Zhiguo Su. High hydrostatic pressure encapsulation of doxorubicin in ferritin nanocages with enhanced efficiency. *Journal of Biotechnology*, 254:34–42, 2017.

[65] Barbara Hennequin, Lyudmila Turyanska, Teresa Ben, Ana M. Beltrán, Sergio I. Molina, Mei Li, Stephen Mann, Amalia Patanè, and Neil R. Thomas. Aqueous near-infrared fluorescent composites based on apoferritin-encapsulated PbS quantum dots. *Advanced Materials*, 20(19):3592–3596, 2008.

[66] Marta Truffi, Luisa Fiandra, Luca Sorrentino, Matteo Monieri, Fabio Corsi, and Serena Mazzucchelli. Ferritin nanocages: A biological platform for drug delivery, imaging and theranostics in cancer. *Pharmacological Research*, 107:57–65, 2016.

[67] Xin Wang, Zhaogang Teng, Haiyan Wang, Chunyan Wang, Ying Liu, Yuxia Tang, Jiang Wu, Jin Sun, Hai Wang, Jiandong Wang, and Guangming Lu. Increasing the cytotoxicity of doxorubicin in breast cancer MCF-7 cells with multidrug resistance using a mesoporous silica nanoparticle drug delivery system. *International Journal of Clinical and Experimental Pathology*, 7(4):1337–1347, 2014.

[68] James E. Lee, Junelina Reed, Malcolm S. Shields, Kathleen M. Spiegel, Larry D. Farrell, and Peter P. Sheridan. Phylogenetic analysis of shiga toxin 1 and shiga toxin 2 genes associated with disease outbreaks. *BMC Microbiology*, 7(1):109, 2007.

[69] Andrew F. Trofa, Hannah Ueno-Olsen, Ruiko Oiwa, and Masanosuke Yoshikawa. Dr. kiyoshi shiga: Discoverer of the dysentery bacillus. *Clinical Infectious Diseases*, 29(5):1303–1306, 1999.

[70] Cheleste M. Thorpe. Shiga toxin producing escherichia coli infection. *Clinical Infectious Diseases*, 38(9):1298–1303, 2004.

[71] Asis Khan, S. C. Das, T. Ramamurthy, A. Sikdar, J. Khanam, S. Yamasaki, Y. Takeda, and G. Balakrish Nair. Antibiotic resistance, virulence gene, and molecular profiles of shiga toxin-producing escherichia coli isolates from diverse sources in calcutta, india. *Journal of Clinical Microbiology*, 40(6):2009–2015, 2002.

[72] Christina R. Hermos, Marcie Janineh, Linda L. Han, and Alexander J. McAdam. Shiga toxin producing escherichia coli in children: Diagnosis and clinical manifestations of o157:h7 and non-o157:h7 infection. *Journal of Clinical Microbiology*, 49(3):955–959, 2011.

[73] M A Karmali, B T Steele, M Petric, and C Lim. Sporadic cases of haemolytic-uraemic syndrome associated with faecal cytotoxin and cytotoxin-producing escherichia coli in stools. *Lancet*, 1(8325):619–620, 1983.

[74] V. L. Tesh and A. D. O'Brien. The pathogenic mechanisms of shiga toxin and the shiga-like toxins. *Molecular Microbiology*, 5(8):1817–1822, 1991.

[75] K. Sandvig. Shiga toxins. *Toxicon*, 39(11):1629–1635, 2001.

[76] Steven A. Mauro and Gerald B. Koudelka. Shiga toxin: Expression, distribution, and its role in the environment. *Toxins*, 3(12):608–625, 2011.

[77] Susanne Hauswaldt, Martin Nitschke, Friedhelm Sayk, Werner Solbach, and Johannes K.-M. Knobloch. Lessons learned from outbreaks of shiga toxin producing escherichia coli. *Current Infectious Disease Reports*, 15(1):4–9, 2013.

[78] C Collins and J.A. Green. A review of the pathophysiology and treatment of shiga toxin producing e. coli infection. *Practical Gastroenterology*, 34:41–50, 2010.

[79] YuJun Cui, DongFang Li, and RuiFu Yang. Shiga toxin-producing escherichia coli o104:h4: An emerging important pathogen in food safety. *Chinese Science Bulletin*, 58(14):1625–1631, 2013.

[80] Piercefield EW, Bradley KK, Coffman RL, and Mallonee SM. HEmolytic uremic syndrome after an escherichia coli o111 outbreak. *Archives of Internal Medicine*, 170(18):1656–1663, 2010.

[81] James C. Paton and Adrienne W. Paton. Pathogenesis and diagnosis of shiga toxin-producing escherichia coli infections. *Clinical Microbiology Reviews*, 11(3):450–479, 1998.

[82] Xiaoping Zhang, Aaron D. McDaniel, Lucas E. Wolf, Gerald T. Keusch, Matthew K. Waldor, and David W. K. Acheson. Quinolone antibiotics induce shiga toxin-encoding bacteriophages, toxin production, and death in mice. *Journal of Infectious Diseases*, 181(2):664–670, 2000.

[83] Yaeta Endo, Kunio Tsurugi, Takashi Yutsudo, Yoshifumi Takeda, Toshihiro Ogasawara, and Kazuei Igarashi. Site of action of a vero toxin (VT2) from escherichia coli o157:h7 and of shiga toxin on eukaryotic ribosomes. *European Journal of Biochemistry*, 171(1):45–50, 1988.

[84] Jon O. Nagy, Yalong Zhang, Wen Yi, Xianwei Liu, Edwin Motari, Jing Catherine Song, Jeffrey T. Lejeune, and Peng George Wang. Glycopolydiacetylene nanoparticles as a chromatic biosensor to detect shiga-like toxin producing escherichia coli o157:h7. *Bioorganic & medicinal chemistry letters*, 18(2):700–703, 2008.

[85] Nikolai Engedal, Tore Skotland, Maria L Torgersen, and Kirsten Sandvig. Shiga toxin and its use in targeted cancer therapy and imaging. *Microbial Biotechnology*, 4(1):32–46, 2011.

[86] Tom G. Obrig. Escherichia coli shiga toxin mechanisms of action in renal disease. *Toxins*, 2(12):2769–2794, 2010.

[87] Ludger Johannes and Winfried Römer. Shiga toxins–from cell biology to biomedical applications. *Nature reviews. Microbiology*, 8(2):105–116, 2010.

[88] Tetsuya Okuda, Noriyo Tokuda, Shin-ichiro Numata, Masafumi Ito, Michio Ohta, Kumiko Kawamura, Joelle Wiels, Takeshi Urano, Orie Tajima, Keiko Furukawa, and Koichi Furukawa. Targeted disruption of gb3/CD77 synthase gene resulted in the complete deletion of globoseries glycosphingolipids and loss of sensitivity to verotoxins. *Journal of Biological Chemistry*, 281(15):10230–10235, 2006.

[89] Niels W. P. Rutjes, Beth A. Binnington, Charles R. Smith, Mark D. Maloney, and Clifford A. Lingwood. Differential tissue targeting and pathogenesis of verotoxins 1 and 2 in the mouse animal model. *Kidney International*, 62(3):832–845, 2002.

[90] Davin Chark, Anita Nutikka, Natasha Trusevych, Julia Kuzmina, and Clifford Lingwood. Differential carbohydrate epitope recognition of globotriaosyl ceramide by verotoxins and a monoclonal antibody. *European journal of biochemistry / FEBS*, 271(2):405–417, 2004.

[91] Mitsumasa Saito, Murugespillai Mylvaganum, Patty Tam, Anton Novak, Beth Binnington, and Clifford Lingwood. Structure-dependent pseudoreceptor intracellular traffic of adamantyl globotriaosyl ceramide mimics. *Journal of Biological Chemistry*, 287(20):16073–16087, 2012.

[92] S Hakomori and Y Zhang. Glycosphingolipid antigens and cancer therapy. *Chemistry & biology*, 4(2):97–104, 1997.

[93] H Farkas-Himsley, R Hill, B Rosen, S Arab, and C A Lingwood. The bacterial colicin active against tumor cells in vitro and in vivo is verotoxin 1. *Proceedings of the National Academy of Sciences of the United States of America*, 92(15):6996–7000, 1995.

[94] Antonio Serna, 4th and Edgar C Boedeker. Pathogenesis and treatment of shiga toxin-producing escherichia coli infections. *Current opinion in gastroenterology*, 24(1):38–47, 2008.

[95] Jinyi Zhao Sulan Bai. Rapid and reliable detection of 11 food-borne pathogens using thin-film biosensor chips. *Applied microbiology and biotechnology*, 86(3):983–90, 2010.

[96] Rambabu Naravaneni and Kaiser Jamil. Rapid detection of food-borne pathogens by using molecular techniques. *Journal of Medical Microbiology*, 54(1):51–54, 2005.

[97] Sowmya Subramanian, Konrad H. Aschenbach, Jennifer P. Evangelista, Mohamed Badaoui Najjar, Wenxia Song, and Romel D. Gomez. Rapid, sensitive and label-free detection of shiga-toxin producing escherichia coli o157 using carbon nanotube biosensors. *Biosensors and Bioelectronics*, 32(1):69–75, 2012.

[98] Heike Margot, Nicole Cernela, Carol Iversen, Claudio Zweifel, and Roger Stephan. Evaluation of seven different commercially available real-time PCR assays for detection of shiga toxin 1 and 2 gene subtypes. *Journal of food protection*, 76(5):871–873, 2013.

[99] K S Kehl, P Havens, C E Behnke, and D W Acheson. Evaluation of the premier EHEC assay for detection of shiga toxin-producing escherichia coli. *Journal of Clinical Microbiology*, 35(8):2051–2054, 1997.

[100] Louise D. Teel, Judy A. Daly, Robert C. Jerris, Diana Maul, Gregory Svanas, Alison D. O'Brien, and Choong H. Park. Rapid detection of shiga toxin-producing escherichia coli by optical immunoassay. *Journal of Clinical Microbiology*, 45(10):3377–3380, 2007.

[101] S Ashkenazi and T G Cleary. Rapid method to detect shiga toxin and shiga-like toxin i based on binding to globotriosyl ceramide (gb3), their natural receptor. *Journal of Clinical Microbiology*, 27(6):1145–1150, 1989.

[102] P. Noguera, G. A. Posthuma-Trumpie, M. van Tuil, F. J. van der Wal, A. de Boer, A. P. H. A. Moers, and A. van Amerongen. Carbon nanoparticles in lateral flow methods to detect genes encoding virulence factors of shiga toxin-producing escherichia coli. *Analytical and Bioanalytical Chemistry*, 399(2):831–838, 2011.

[103] Jianling Wang, Guihua Chen, Hui Jiang, Zhiyong Li, and Xuemei Wang. Advances in nano-scaled biosensors for biomedical applications. *Analyst*, 138(16):4427–4435, July 2013.

[104] Amit Singh, Somayyeh Poshtiban, and Stephane Evoy. Recent advances in bacteriophage based biosensors for food-borne pathogen detection. *Sensors*, 13(2):1763–1786, 2013.

[105] Takehiro Nagatsuka, Hirotaka Uzawa, Keita Sato, Satoshi Kondo, Masayuki Izumi, Kenji Yokoyama, Isaac Ohsawa, Yasuo Seto, Paola Neri, Hiroshi Mori, Yoshihiro Nishida, Masato Saito, and Eiichi Tamiya. Localized surface plasmon resonance detection of biological toxins using cell surface oligosaccharides on glyco chips. *ACS Applied Materials & Interfaces*, 5(10):4173–4180, 2013.

[106] Shu-I Tu, Tao Geng, Joe Uknalis, and Arun Bhunia. Fiber-optic biosensor employing alexa-fluor conjugated antibodies for detection of escherichia coli o157:h7 and shiga-like toxins. volume 6381, pages 638106–638106–6, 2006.

[107] Miriam M. Ngundi, Chris R. Taitt, Scott A. McMurry, Daniel Kahne, and Frances S. Ligler. Detection of bacterial toxins with monosaccharide arrays. *Biosensors and Bioelectronics*, 21(7):1195–1201, 2006.